Dalton Transactions

ROYAL SOCIETY OF CHEMISTRY

PAPER

View Article Online
View Journal | View Issue

Cite this: *Dalton Trans.*, 2025, **54**, 5367

Water-soluble luminescent platinum(II) complexes for guanine quadruplex binding†

Simon Kroos,[a] Marian Hebenbrock,[a] Alexander Hepp,[a] Marcus Layh,[a] Joschua Lüke,[a,b] Ali R. Tonkul,[a] Cristian A. Strassert[a,b,c] and Jens Müller *[a,c]

A family of 16 platinum(II) complexes was synthesized with the aim of obtaining water-soluble luminescent coordination compounds for guanine quadruplex (G4) binding. The complexes share a common tridentate N^N^C-donor ligand (based on 2-phenyl-6-(1*H*-1,2,3-triazol-4-yl)pyridine) bearing different substituents for solubilization, and an additional monodentate ancillary ligand (either phenylacetylide or 3-(trimethylammonium)prop-1-yne-1-ide). Single-crystal X-ray diffraction analyses confirm that the substituents do not interfere with the central planar core of the complexes required for π stacking interactions with the DNA. The interaction of the complexes with four DNA oligonucleotides that fold into various G4 topologies was evaluated using luminescence and circular dichroism spectroscopy as well as cryo-ESI mass spectrometry. The data indicate a complex correlation between type of substituent and ability of the complex to interact with G4 DNA.

Received 1st November 2024,
Accepted 24th February 2025

DOI: 10.1039/d4dt03067b

rsc.li/dalton

Introduction

Guanine-rich DNA sequences, which are ubiquitous in the genome, can fold into tetra-stranded helical structures, so-called guanine quadruplexes (G4). G4 consist of guanine tetrads, each of which comprises four guanine residues arranged in a planar pattern, assembled *via* Watson–Crick and Hoogsteen hydrogen bonding. The G quadruplexes are further stabilized by electrostatic interactions with monovalent cations. K(I) coordinates between two G tetrads, whereas Na(I) mostly coordinates in the plane of a G tetrad (Chart 1).[1,2]

G4 structures form in guanine-rich nucleic acid sequences, which occur in human telomeres, in various oncogene promoter regions, and in non-human genomes as well as in artificial sequences proposed to be relevant in biological mechanisms.[3–5] The sequences can adopt different topologies with parallel, antiparallel and hybrid strand orientation.[6,7] Telomeres contain a repetitive overhang at the 3′ end of eukaryotic chromosomes, in humans composed of the repeating hexanucleotide sequence $d(TTAGGG)_n$.[8] This overhang plays an important role in the control of cell replication and cell division.[9] In healthy cells, replication leads to incomplete duplication and the resulting shortening of the telomere sequence. At a critical telomere length, apoptosis is initiated. In 80% of cancer cells, the enzyme telomerase is overexpressed, preventing apoptosis.[10,11] The formation of G quadruplexes in the telomere region can inhibit telomerase and thus represents an elegant target for research into new cancer therapeutics.[12,13] Likewise, the targeting of G4 in a promoter region is known to be able to suppress the transcription of the respective gene.[14] Here, G4 formation is typically suppressed

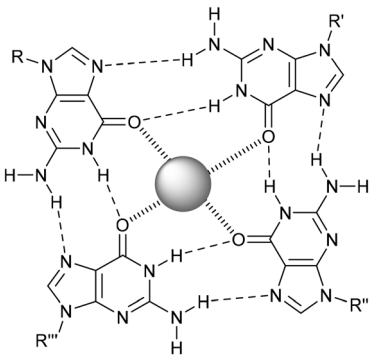

Chart 1 Formation of a guanine tetrad *via* hydrogen bonds. The grey sphere represents a central cation.

[a]*Universität Münster, Institut für Anorganische und Analytische Chemie, Corrensstr. 28/30, 48149 Münster, Germany. E-mail: mueller.j@uni-muenster.de*
[b]*Universität Münster, Center for Nanotechnology (CeNTech), Heisenbergstr. 11, 48149 Münster, Germany*
[c]*Universität Münster, Center for Soft Nanoscience (SoN) and Cells in Motion Interfaculty Centre (CiMIC), Corrensstr. 28/30, 48149 Münster, Germany*

†Electronic supplementary information (ESI) available: Crystallographic data, molecular polarity index, UV/Vis spectra, emission spectra, time-resolved photoluminescence decay curves with fitting parameters; CD spectra, melting curves, TO displacement assays, HPLC chromatograms, NMR spectra. CCDC 2392538–2392541. For ESI and crystallographic data in CIF or other electronic format see DOI: **https://doi.org/10.1039/d4dt03067b**

under normal conditions, due to duplex formation. However, molecular crowding or negative superhelicity during transcription can enhance G4 formation,[15] as can the addition of suitable small molecules. Hence, the induction and stabilization of G quadruplexes in promoter regions is also an attractive research area in cancer therapy.

Among the molecules that can target quadruplexes, a variety of heteroaromatic ligands have been reported.[16–18] They interact through external π stacking, making use of their large aromatic surface, *e.g.*, in porphyrin- or pyrene-based molecules.[19,20] Metal complexes based on the salen chelator were also proposed as attractive potential G4 binders.[21] They offer the additional possibility of extending the positively charged channel along the G4 helical axis.[22,23] A number of metal complexes were investigated as G4 binders, including Mn(II),[24,25] Ni(II),[26] Cu(II),[1] Pd(II),[27] Ru(II),[28,29] Au(I),[30] Ir(III),[31] and Pt(II) complexes.[1,24,26,32–34] In these complexes, the ligand type goes well beyond that of a salen-based scaffold.

Recently, we showed that attaching a pendant nucleobase to the tridentate N^N^C ligand of a phosphorescent Pt(II) complex structurally related to the ligand under investigation in this project led to unique binding properties with respect to G quadruplexes.[35] However, those complexes were not water-soluble and quite bulky. In the present study, luminescent Pt(II) complexes with a tridentate ligand, either mono- or difunctionalized, possibly containing a cationic pendant group, and a sterically non-demanding monodentate auxiliary ligand are investigated (Chart 2). Earlier studies on closely related complexes had shown that they are phosphorescent,[36–38] which renders them interesting in the context of a time-gated imaging. Those studies also indicated that the identity of the auxiliary monodentate ligand hardly influences the phosphorescence of the Pt(II) complexes.[36] Hence, it can be expected that the use of a sterically non-demanding monodentate ligand in the present study neither affects the phosphorescent properties.

The development of luminescent G4 binders is of particular interest, because they often function as luminescence "turn-on" probes upon interaction with a nucleic acid,[34,39,40] allowing visualization of DNA even in cells.[33,41] Alternatively (or additionally), a change in luminescence lifetime may be used to detect an interaction with G4 DNA.[33,42,43] The light-switch effect occurring upon interaction of a potentially luminescent compound with a nucleic acid is based on the deactivation of the excited state by water. When interacting with a nucleic acid, the compound is shielded from the solvent and its intrinsic luminescence is restored.[44]

In the present study the combination of an enlarged π system and the possibility of engaging in hydrogen bonding interactions involving the pendant groups and the auxiliary ligand was expected to lead to a better target selectivity. A particular focus is given to the functionalization of the tridentate ligand, aiming at a high water-solubility of the final complex. The interaction of this family of Pt(II) complexes with four distinct G4 DNA structures was investigated by circular dichroism (CD) spectroscopy, a Förster resonance energy transfer (FRET) based melting assay, fluorescence intercalator displacement studies, and isothermal titration calorimetry (ITC).

Due to the structural complexity of the ligands and metal complexes presented herein, the IUPAC nomenclature was replaced by an independent simplified labelling. In this context, the monodentate auxiliary ligands phenylacetylide and 3-(trimethylammonium)prop-1-yne-1-ide are termed A and B, respectively. The functional groups attached to the ligand precursor (LH) are represented by superscript abbreviations, depending on the substituent(s): 3-chloropropyl (Cl), 3-bromopropyl (Br), 3-hydroxypropyl (OH), 3-morpholinopropyl (M), phosphate ester (P).

The four quadruplex-forming sequences H-telo, *c-myc22*, *bcl2*-mid and *c-kit* were selected for this study. They all contain three stacked guanine tetrads but adopt different topologies, they were structurally characterized, and are potential therapeutic targets. In particular, H-telo is based on the human telomeric repeat sequence d(TTAGGG). It can adopt various topologies depending on experimental conditions. Under the conditions applied in this study, it forms a hybrid structure with parallel and antiparallel strand orientation and a characteristic T : A : T cap.[45] The other three sequences are derived from the promotor regions of the genes *c-MYC*, *BCL2*, and *c-KIT*. *c-MYC* is an oncogene that can be silenced *via* the for-

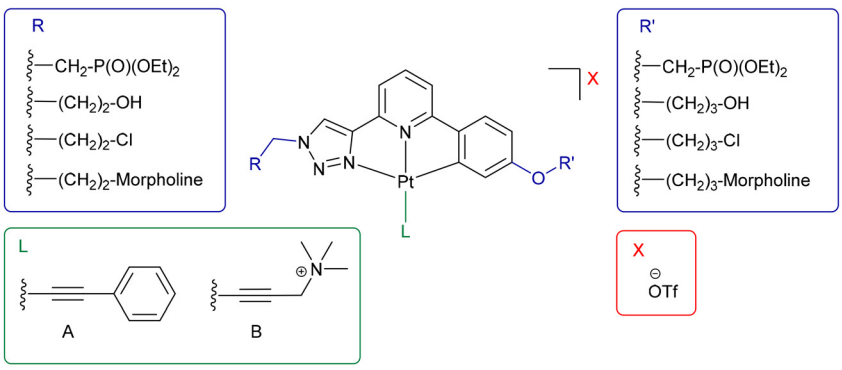

Chart 2 Structural composition of the Pt(II) complexes. The basic structure of the ligand (black), the functionalization sites R and OR′ (blue), the auxiliary ligand L to be varied (green), and the respective counterion (red) are highlighted in a color code.

mation of a G4 structure in its promotor region.[46] The *c-myc22* sequence investigated here is a double mutant (*c-myc*22-G14T/G23T) known to adopt a parallel fold.[2] The *bcl2*-mid sequence represents a truncated and partially mutated excerpt from the promotor region of the human *BCL2* gene. It adopts a hybrid structure under the experimental conditions used here.[47] Finally, *c-KIT* is a proto-oncogene with a guanine-rich promotor region. The *c-kit* sequence investigated here (also referred to as *c-kit87up* because it is located 87 nucleotides upstream of the transcription start site) adopts a parallel fold.[48] A peculiarity of this structure is the fact that it contains an isolated guanosine in one of the tetrads, whereas these are normally formed from three-guanine tracts. An overview of the structures is given in Fig. 1.

Results and discussion

Synthesis of the ligand precursors

The synthesis of all ligand precursors starts from 2-ethynyl-6-phenylpyridine **1** (Scheme 1). This compound was previously reported by Hebenbrock *et al.*[36] In three independent reactions, **1** was converted with diethyl (2-azidoethyl)phosphonate, 4-(3-azidopropyl)morpholine, and 3-azidopropan-1-ol to give

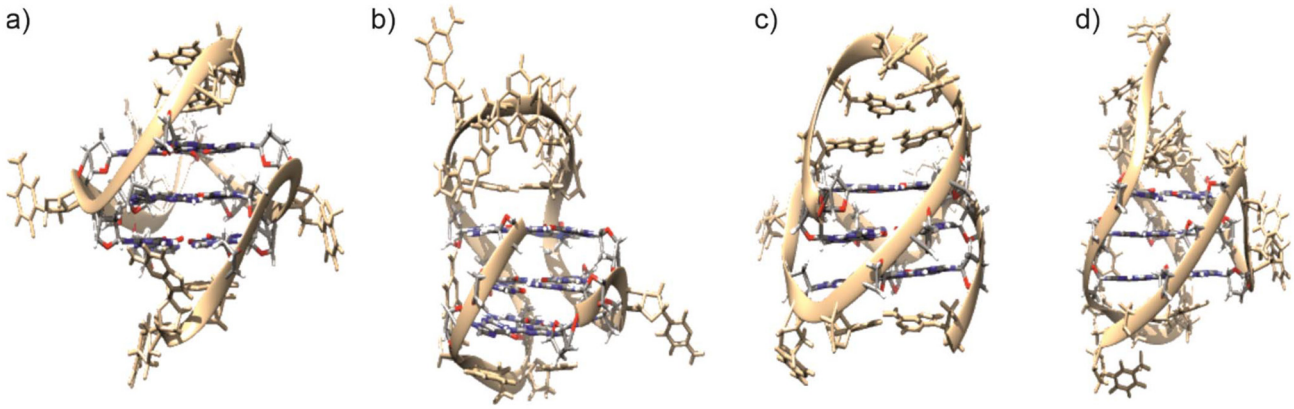

Fig. 1 Experimental structures of the G4 sequences used in this study as previously reported for K^+-containing solutions. (a) *c-myc22*,[2] (b) *bcl2*-mid,[47] (c) *c-kit*,[48] (d) H-telo.[45] This figure was created using UCSF Chimera[49] and is reprinted from reference.[50] The structures were obtained from the PDB accession codes 1XAV, 2F8U, 2O3M, and 2JPZ, respectively.

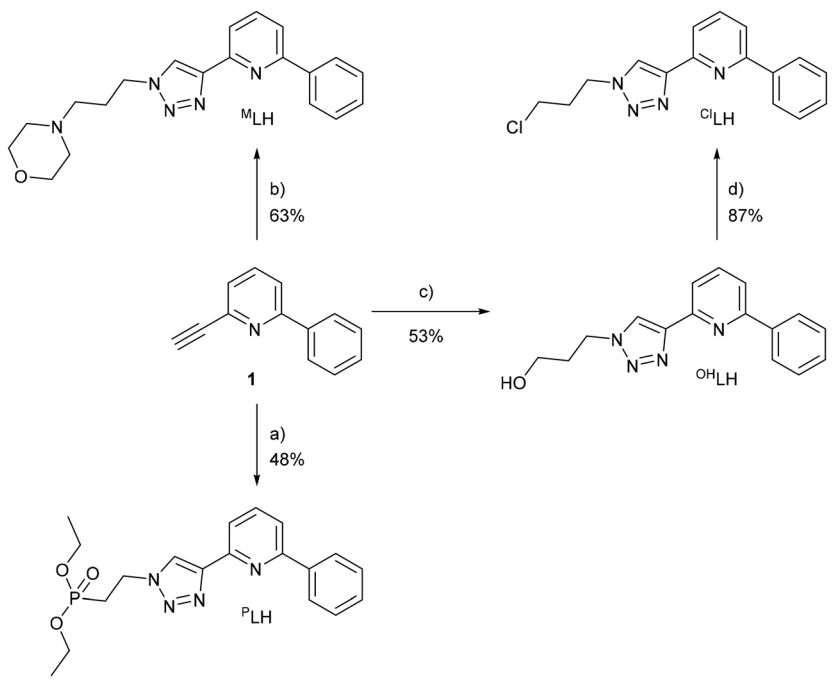

Scheme 1 a) Diethyl (2-azidoethyl)phosphonate, general procedure for click reaction; (b) 4-(3-azidopropyl)morpholine, general procedure for click reaction; (c) 3-azidopropan-1-ol, general procedure for the click reaction; (d) $SOCl_2$, CH_2Cl_2, 0 °C, o/n.

compounds ^{P}LH, ^{M}LH, and ^{OH}LH, respectively. ^{OH}LH was subsequently converted to the chloroalkyl-containing ligand precursor ^{Cl}LH by direct reaction of the hydroxy functionality with thionyl chloride.

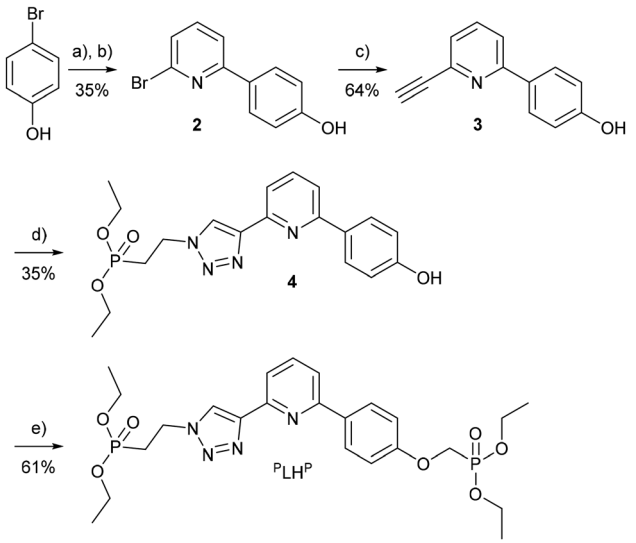

Scheme 2 a) 3,4-Dihydro-2*H*-pyran, HCl, rt, 2 h; (b) (1) ^{n}BuLi, B(O^{i}Pr)$_3$, −78 °C, dry THF; (2) 2,6-dibromopyridine, K_2CO_3, PPh_3, $Pd(OAc)_2$, 1,2-dimethoxyethane, H_2O, 110 °C, 18 h; (c) (1) TMS acetylene, CuI, $[PdCl_2(PPh_3)_2]$, dry THF, dry NEt_3, 80 °C, o/n; (2) NaOH (1 M), THF, MeOH, rt, 2 h; (d) diethyl (2-azidoethyl)phosphonate, general procedure for the click reaction; (e) (diethyl phosphoric) trifluoromethanesulfonic anhydride, K_2CO_3, ACN, 18 h, reflux.

The difunctionalized ligand precursors were synthesized starting from 4-bromophenol. Initially, 4-bromophenol was protected with 3,4-dihydro-2*H*-pyran in an acid-catalysed reaction.[51] It was then transformed into a boronic acid by bromine lithium exchange and reaction with triisopropyl borate. Finally, a Suzuki cross-coupling reaction with 2,6-dibromopyridine followed by cleavage of the tetrahydropyranyl ether (under acidic conditions by means of concentrated hydrochloric acid) gave compound **2** in two steps (Scheme 2).[52] In a Sonogashira cross-coupling reaction, compound **2** was reacted with trimethylsilyl acetylene. 4-(6-Ethynylpyridin-2-yl)phenol **3** was obtained after cleavage of the silyl protecting group under basic conditions. To access the diphosphate ester ligand precursor ^{P}LH^{P}, intermediate **4** was formed from compound **3** and diethyl (2-azidoethyl)phosphonate in a Cu(I)-catalysed Huisgen reaction. Subsequently, the phenolic hydroxy group was functionalized to give ^{P}LH^{P}.

To increase the diversity of difunctionalized ligand precursors, the phenolic hydroxy group of compound **2** was functionalized with 3-chloropropan-1-ol in the presence of K_2CO_3 and CuI (for halogen exchange on 3-chloropropan-1-ol to increase the leaving-group capability) to give intermediate **5** (Scheme 3).[53] A Sonogashira cross-coupling reaction with trimethylsilyl acetylene and subsequent deprotection under basic conditions with aqueous NaOH solution yielded compound **6**. As reported above for the monofunctionalized ligand precursor ^{OH}LH, a Cu(I)-catalysed Huisgen reaction with 3-azidopropan-1-ol resulted in the formation of the ligand precursor ^{OH}LH^{OH}. Starting from ^{OH}LH^{OH}, the dichlorinated species ^{Cl}LH^{Cl} was synthesized by means of thionyl chloride, and the dibromi-

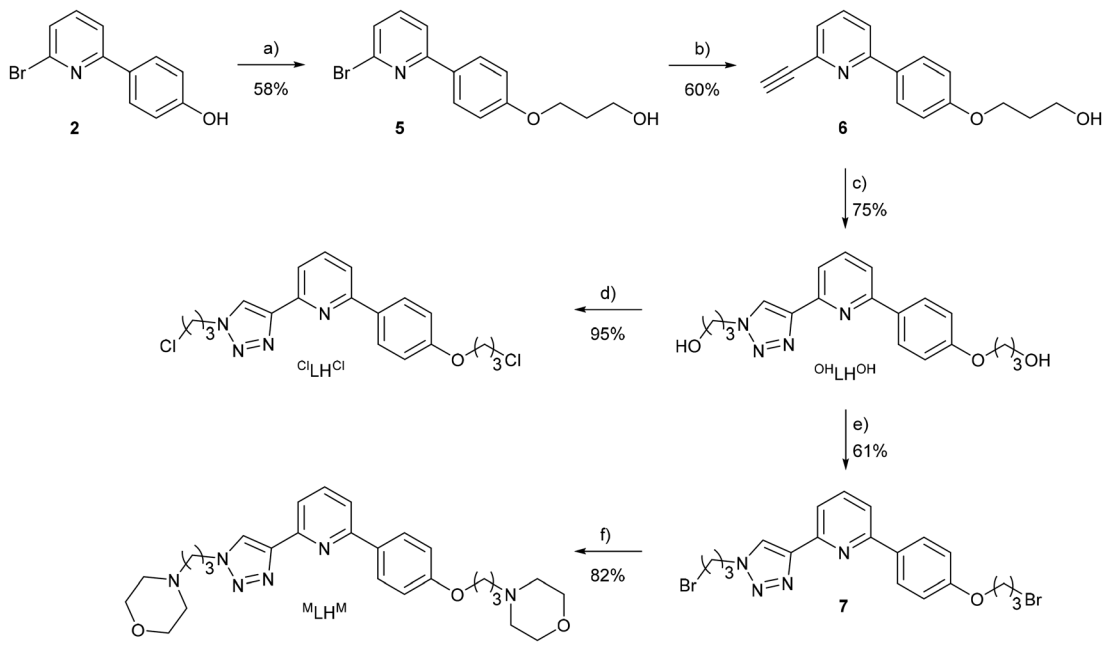

Scheme 3 a) K_2CO_3, CuI, 3-chloropropan-1ol, 3 d, reflux; (b) (1) TMS acetylene, CuI, $[PdCl_2(PPh_3)_2]$, dry THF, dry NEt_3, 80 °C, o/n; (2) NaOH (1 M), THF, MeOH, rt, 2 h; (c) 3-azidopropan-1-ol, $CuSO_4{\cdot}5\ H_2O$, Na ascorbate, ^{t}BuOH, H_2O, THF, rt, o/n; (d) $SOCl_2$, CH_2Cl_2, 0 °C, o/n; (e) PPh_3, *N*-bromosuccinimide, dry DCM, 0 °C, o/n; (f) morpholine, K_2CO_3, ACN, reflux, o/n.

nated species 7 with *N*-bromosuccinimide. Starting from compound 7, ligand precursor $^{M}LH^{M}$ containing two pendant morpholine moieties was obtained by nucleophilic substitution with morpholine in the presence of K_2CO_3. Under physiological pH conditions, this compound is expected to be protonated and thereby converted into a cation.

Synthesis of the platinum(II) complexes

The complexation with Pt(II) was carried out by employing K_2PtCl_4 in boiling acetic acid under an inert atmosphere to obtain [PtCl(^{M}L)] and [PtCl($^{M}L^{M}$)]. For the syntheses of the other complexes, a mixture of water and 2-ethoxyethanol was used as solvent.[54] The ancillary chlorido ligand was easily exchanged either *via* a salt elimination reaction with silver phenylacetylide or by a Sonogashira-like transfer of *N*,*N*,*N*-trimethyl-*N*-propargylammonium triflate.

Molecular structures of selected platinum complexes

Molecular structures were determined for [Pt(A)(^{M}L)] and [Pt(A)(^{Cl}L)] using single-crystal X-ray diffraction analysis (see ESI, Table S1,† for crystallographic details). As can be seen from Fig. 2a and b, the substituents do not interfere with the central planar core of the complexes required for π stacking interactions with G4 DNA (in contrast to the behaviour seen in a related earlier study).[35] The phenyl moiety of the ancillary phenylacetylido ligand it oriented almost perpendicular with respect to the square-planar coordination environment of the Pt(II) ion (62.8(1)° and 79.71(5)°, respectively). Hence, it can be speculated that this moiety may serve as some kind of anchor when the complex binds non-covalently to G4 DNA. In case of the complexes with disubstituted ligands, molecular structures were determined for the intermediates [PtCl($^{P}L^{P}$)] and [PtCl($^{OH}L^{OH}$)] bearing a chlorido ancillary ligand (Fig. 2c and d). These complexes were not evaluated with respect to their ability to bind non-covalently to DNA because chlorido ligands are known to dissociate from Pt(II) complexes, enabling the (at this point undesired) formation of Pt–DNA bonds.[55] Nevertheless, the complexes represent valid structural models for the corresponding complexes with ancillary ligands A and B. Hence, it can be concluded that again the substituents do not interfere with the central planar core of the complexes required for π stacking interactions with G4 DNA. Table 1 presents an overview of bond lengths involving the Pt(II) ion. These bond lengths are in the expected range.[56]

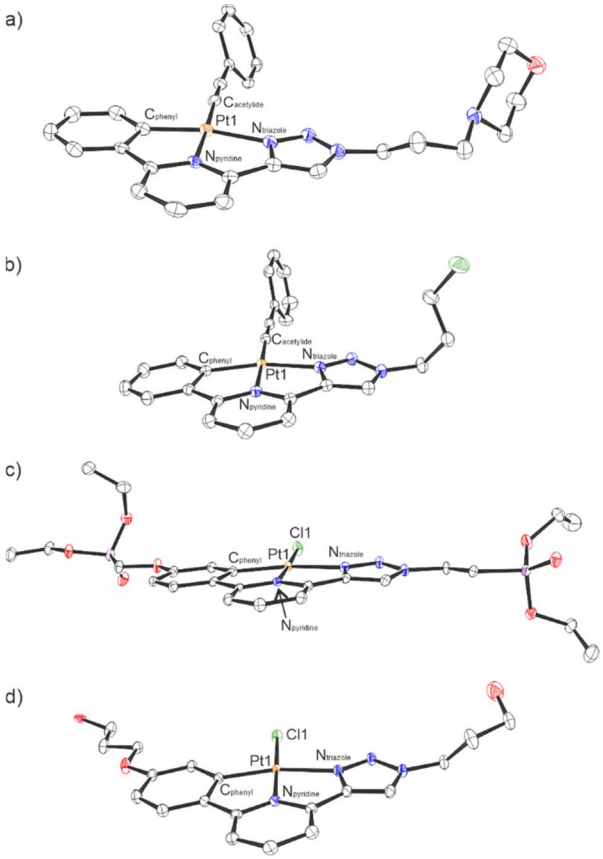

Fig. 2 Molecular structures of (a) [Pt(A)(^{M}L)], (b) [Pt(A)(^{Cl}L)] (a co-crystallized CH_2Cl_2 molecule is omitted for clarity), (c) [PtCl($^{P}L^{P}$)], and (d) [PtCl($^{OH}L^{OH}$)] (a co-crystalized DMF molecule (half a molecule in the asymmetric unit) is omitted for clarity) in the crystal. Displacement ellipsoids are drawn at the 50% probability level. H atoms are omitted for clarity.

Table 1 Selected bond lengths/Å in the molecular structures of the Pt(II) complexes

Compound	Pt1–$N_{triazole}$	Pt1–$N_{pyridine}$	Pt1–C_{phenyl}	Pt1–X
[Pt(A)(^{M}L)]	2.119(6)	2.011(5)	1.992(7)	1.961(6)[a]
[Pt(A)(^{Cl}L)]	2.102(1)	2.005(1)	1.986(2)	1.962(2)[a]
[PtCl($^{P}L^{P}$)]	2.120(2)	1.969(2)	1.978(3)	2.3073(7)[b]
[PtCl($^{OH}L^{OH}$)]	2.124(2)	1.967(2)	1.984(2)	2.3048(4)[b]

[a] X = $C_{acetylide}$. [b] X = Cl1.

DFT calculations

To correlate the ability of the various complexes to engage in intermolecular interactions with their structural composition, the charge balance parameter ν (ranging from 0.000 to 0.250) was determined by means of DFT calculations.[57,58] A large ν value indicates a tendency for engaging in an intermolecular interaction involving both the positive and negative regions to a similar extent. For the complexes functionalized with morpholine, the respective protonated complexes were also evaluated. Direct comparison of the ν values as a function of auxiliary ligands A and B (or of the charge density) reveals a clear trend. Auxiliary ligand A appears to strongly promote intermolecular interactions between individual complexes. With ν values between 0.227 and 0.250, an intermolecular interaction is clearly preferred compared to complexes with the auxiliary ligand B, which have ν values of merely 0.000 to 0.035. In addition to the auxiliary ligand, the charge of the complex plays a central role. The complexes with auxiliary ligand A and bearing a protonated morpholine moiety display a ν value between 0.000 and 0.015 and hence do not favour intermolecular interactions. Finally, in addition to the auxiliary

ligand and the charge of the complex, the steric demand plays an important role. With increasing steric demand, the ν value decreases from 0.250 for [Pt(A)(^{Cl}L^{Cl})] to 0.227 for [Pt(A)(^{P}L^{P})] within the family of complexes with the auxiliary ligand A (Table 2). In summary, these data suggest that complexes bearing this auxiliary ligand are more likely to aggregate in solution.

To complement this insight, the molecular polarity index (MPI) was calculated for each complex. The MPI clearly correlates with the charge of the complex (see ESI, Table S2†). Moreover, complexes with auxiliary ligand A have a smaller MPI than the respective complexes with auxiliary ligand B, indicating the increased polarity in the latter case. In general, these data suggest that the complexes should be soluble in polar solvents. In fact, complexes bearing auxiliary ligand A turned out to be soluble in DMSO, whereas complexes with auxiliary ligand B were sufficiently water-soluble to prepare 750 μM aqueous stock solutions (except for [Pt(B)(^{OH}L^{OH})]OTf, which was soluble in DMSO).

UV/vis spectroscopic and photoluminescence studies of the complexes

All complexes were characterized by UV/vis absorption and photoluminescence spectroscopies (λ_{exc} = 340 nm) to study their possible aggregation in concentrated solutions. The complexes absorb strongly in the wavelength region from 240–400 nm (see ESI, Fig. S1 and S2†). Based on the results obtained for closely related complexes, the absorbance around 270 nm can be attributed to allowed transitions into $^{1}\pi$–π^* states, whereas the bands at 300–400 nm are attributed to the excitation into mixed ^{1}MLCT/LC states.[36,59–62]

As anticipated from earlier studies on closely related complexes bearing an unsubstituted tridentate ligand,[35–38] the Pt(II) complexes are luminescent (see ESI, Fig. S3–S10†). They show an emission band centring around 500 nm with vibrational progression at longer wavelengths. Fig. 3 exemplarily displays concentration-dependent luminescence spectra of [Pt(A)(^{M}L)]. At low concentrations, the main emission band at 500 nm and its vibrational progression are clearly discernible. For [Pt(A)(^{M}L)] and a few other complexes, the formation of aggregates in aqueous solution at concentrations >15 μM can be deduced from the appearance of an additional broad red-shifted emission band at *ca.* 620 nm, attributed to ^{3}MMLCT states. For some complexes, an additional emission band at *ca.* 400 nm is observed (*vide infra*). A general observation is that the identity of the auxiliary monodentate ligands hardly influences the luminescence of the complexes, thereby extending this observation to complexes with different substitution patterns on the tridentate ligand.

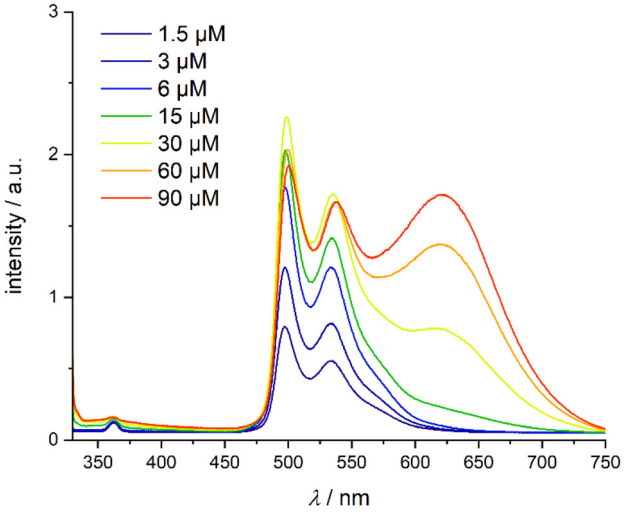

Fig. 3 Concentration-dependent emission spectra of [Pt(A)(^{M}L)]. Conditions: metal complex (1.5–90 μM), 20 °C, λ_{exc} = 340 nm.

With a potential application as probe for G4 structures in mind, the photoluminescence quantum yields of the complexes were determined. Almost all complexes bearing the auxiliary ligand A had to be dissolved in DMSO to reach the concentration necessary for performing these measurements. As a result, their quantum yields could not be determined due to quenching by the solvent. As can be seen from the overview given in Table 3, the quantum yields of the other complexes in deaerated water reach up to 36%, rendering the compounds interesting for imaging applications.

In general, the experimental luminescence-spectroscopic data obtained for the monofunctionalized complexes agree well with the conclusions drawn from the calculated ν values. Unexpectedly, among the monofunctionalized complexes bearing auxiliary ligand B, the compound [Pt(B)(^{P}L)]OTf does aggregate to a certain extent under the experimental conditions (see ESI, Fig. S10†), contrasting theoretical expectations (ν = 0.011). In all other cases, the quaternary amine with its positive charge prevents the aggregation of the metal complexes with auxiliary ligand B when compared to the corresponding complexes bearing auxiliary ligand A (see ESI, Fig. S3–S10†).

An aggregation was not observed experimentally for the difunctionalized complexes, which is in agreement with computational predictions. Among these complexes, merely [Pt(A)(^{Cl}L^{Cl})] self-aggregates, as deduced from the pronounced absorbance at >600 nm, even though there is a decrease in intensity when increasing the concentration beyond 60 μM.

Table 2 ν values of the complexes as determined by DFT calculations, including color-coded heat map

Complex	ν	Complex	ν
[Pt(A)(^{Cl}L)]	0.250	[Pt(B)(^{Cl}L)]$^{+}$	0.000
[Pt(A)(^{Cl}L^{Cl})]	0.250	[Pt(B)(^{Cl}L^{Cl})]$^{+}$	0.000
[Pt(A)(^{M}L)]	0.246	[Pt(B)(^{M}L)]$^{+}$	0.005
[Pt(A)(^{MH}L)]$^{+}$	0.015	[Pt(B)(^{MH}L)]$^{2+}$	0.000
[Pt(A)(^{M}L^{M})]	0.238	[Pt(B)(^{M}L^{M})]$^{+}$	0.035
[Pt(A)(^{MH}L^{MH})]$^{2+}$	0.000	[Pt(B)(^{MH}L^{MH})]$^{3+}$	0.000
[Pt(A)(^{OH}L)]	0.248	[Pt(B)(^{OH}L)]$^{+}$	0.000
[Pt(A)(^{OH}L^{OH})]	0.241	[Pt(B)(^{OH}L^{OH})]$^{+}$	0.000
[Pt(A)(^{P}L)]	0.239	[Pt(B)(^{P}L)]$^{+}$	0.011
[Pt(A)(^{P}L^{P})]	0.227	[Pt(B)(^{P}L^{P})]$^{+}$	0.047

0.000 0.250

Table 3 Overview of photoluminescence quantum yields (Φ_{PL})[a]

Compound	Φ_{PL}/air	Φ_{PL}/Ar
[Pt(A)(^{Cl}L)][b]	<2	<2
[Pt(A)(^{Cl}L^{Cl})][b]	<2	<2
[Pt(A)(^{M}L)][b]	<2	<2
[Pt(A)(^{M}L^{M})][b]	<2	<2
[Pt(A)(^{OH}L)][b]	<2	<2
[Pt(A)(^{OH}L^{OH})][c]	3 ± 2	14 ± 2
[Pt(A)(^{P}L)][b]	<2	<2
[Pt(A)(^{P}L^{P})][b]	<2	<2
[Pt(B)(^{Cl}L)]OTf[d]	4 ± 2	35 ± 4
[Pt(B)(^{Cl}L^{Cl})]OTf[d]	4 ± 2	18 ± 2
[Pt(B)(^{M}L)]OTf[d]	3 ± 2	25 ± 3
[Pt(B)(^{M}L^{M})]OTf	n.d.[e]	n.d.[e]
[Pt(B)(^{OH}L)]OTf[d]	4 ± 2	28 ± 3
[Pt(B)(^{OH}L^{OH})]OTf[d]	<2	20 ± 2
[Pt(B)(^{P}L)]OTf[d]	6 ± 2	36 ± 4
[Pt(B)(^{P}L^{P})]OTf[d]	3 ± 2	32 ± 3

[a] Conditions: Ar atmosphere, λ_{exc} = 350 nm. [b] Measured in DMSO. [c] Measured in a 10% DMSO aqueous solution. [d] Measured in water. [e] Not determined.

Surprisingly, a further prominent emission band at *ca.* 400 nm is detected for all difunctionalized Pt(II) complexes bearing auxiliary ligand A, growing in intensity with increasing concentration and partially overlapping with the band of the Raman scattering of water at 362 nm (see ESI, Fig. S3–S10†). To understand whether this emission is an intrinsic property of the metal complexes or whether it is caused by the presence of residual amounts of an unknown impurity, the Pt(II)-free ligand precursors were also evaluated with respect to their emission properties, applying the maximum concentration of 90 μM used in the complex studies. Their spectra (see ESI, Fig. S11–S14†) show that the monodentate ligand precursors do not luminesce, whereas the difunctionalized ones weakly emit at *ca.* 400 nm, with the emission in part being superimposed by the excitation (λ_{exc} = 340 nm). While this could imply the presence of small amounts of unreacted ligand precursor in the samples of the difunctionalized metal complexes, it does not explain that the appearance of the emission band at *ca.* 400 nm can in some cases also be evoked by the addition of G4 DNA (*vide infra*). Moreover, the complexes are pure as evidenced by NMR spectroscopy and elemental analysis. Time-dependent ^{1}H NMR spectroscopy also confirms their stability in solution for several days (see ESI, Fig. S15–S28†), ruling out any decomposition or a possible adduct formation. Hence, the source of the unexpected emission at *ca.* 400 nm remains unclear for the time being.

Photoluminescence studies of the complexes in the presence of G4 DNA

The water-soluble Pt(II) complexes were developed as potential agents for the visualization of G4 DNA. Therefore, their photoluminescence spectra in the presence of the G4 DNA and dsDNA (ds26, acting as a double-stranded reference) were investigated. In most cases, the addition of an oligonucleotide to the complex leads to an increase in its luminescence at *ca.* 500 nm (Fig. 4; see ESI, Fig. S29–S44† for a compilation of all data). Table 4 gives an overview of the increase in luminescence intensity induced by the presence of the respective oligonucleotide. Neither the identity/number of the substituents on the tridentate nor the identity of the auxiliary monodentate ligand appears to correlate with the luminescence change. Nevertheless, the following observations can be made. The emission of [Pt(A)(^{Cl}L)] and [Pt(A)(^{Cl}L^{Cl})] is particularly influenced by *c-mcy22* and *bcl2*-mid, whereas that of [Pt(A)(^{M}L^{M})] increases significantly in the presence of any of the investigated oligonucleotides. The luminescence of [Pt(B)(^{P}L)]OTf is particularly strongly influenced by H-telo. Among the G4 quadruplexes investigated here, *c-kit* is the one with the smallest effect on the luminescence of the Pt(II) complexes and merely increasing the luminescence of [Pt(A)(^{M}L^{M})] and [Pt(B)(^{P}L)]OTf.

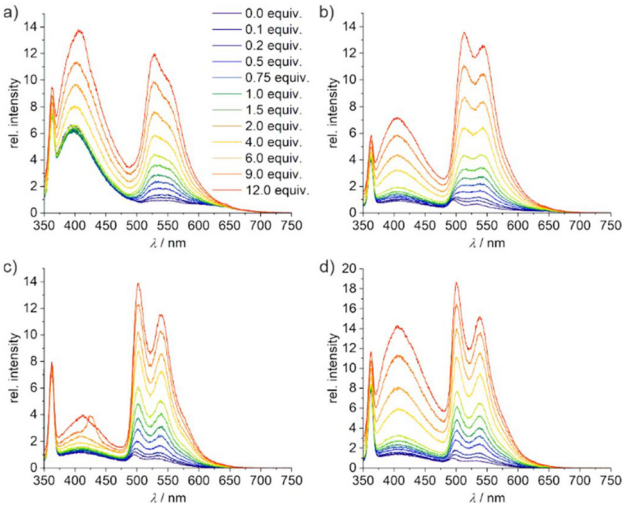

Fig. 4 Emission spectra of (a) [Pt(A)(^{Cl}L^{Cl})] and (b) [Pt(A)(^{Cl}L)] upon stepwise addition of *c-myc22* (0–12 equiv.). Emission spectrum of [Pt(B)(^{OH}L)]OTf upon stepwise addition of (c) *c-kit* and (d) H-Telo (0–12 equiv.). Conditions: metal complex (1 μM), LiCl (90 mM), KCl (10 mM), MOPS (5 mM, pH 7.4), 20 °C, λ_{exc} = 340 nm.

Interestingly, the addition of DNA in most instances evokes the appearance of a new emission band at *ca.* 400 nm, similar to the unexpected emission seen for all difunctionalized Pt(II) complexes bearing auxiliary ligand A (*vide supra*). However, here the presence of this band is not limited to these Pt(II) complexes but also appears for monofunctionalized complexes and for complexes with auxiliary ligand B. While *c-kit* again exerts the least influence, ds26 is affecting the luminescence of almost all complexes at *ca.* 400 nm.

Further experiments were carried out to characterize the relevant emission bands at *ca.* 400 nm and at >500 nm in more detail. For this purpose, the emission spectra of selected complexes were recorded in the absence and presence of *bcl2*-mid. This sequence was selected out of the four quadruplexes because it shows relevant interactions with several of the complexes when taking into consideration all characterization methods applied in this study. An excited state lifetime in the

Table 4 Heatmap illustrating the change in luminescence of the Pt(II) complexes as a function of the added oligonucleotide (12 equiv.)[a]

Complex	*c-myc22*		*bcl2*-mid		*c-kit*		H-telo		ds26	
	[b]	[c]	[b]	[c]	[b]	[c]	[b]	[c]	[b]	[c]
[Pt(A)(^{Cl}L)]	7.9	9.5	8.9	11.6	1.9	2.0	9.0	2.4	19.7	2.1
[Pt(B)(^{Cl}L)]OTf	7.7	3.6	8.1	4.4	2.1	1.9	9.6	2.4	22.8	1.9
[Pt(A)(^{Cl}L^{Cl})]	2.0	12.4	1.6	6.9	0.9	3.0	2.1	3.9	4.0	3.4
[Pt(B)(^{Cl}L^{Cl})]OTf	7.0	4.3	6.7	3.9	1.9	3.2	6.9	4.0	12.8	1.7
[Pt(A)(^{M}L)]	9.5	0.8	9.1	1.9	2.1	0.6	8.9	1.0	19.9	0.7
[Pt(B)(^{M}L)]OTf	10.8	3.7	10.1	3.4	2.6	2.3	9.4	2.6	24.8	1.7
[Pt(A)(^{M}L^{M})]	5.1	19.1	9.9	10.4	1.4	11.8	4.8	15.5	9.9	10.4
[Pt(B)(^{M}L^{M})]OTf	7.0	6.2	7.0	6.2	2.3	5.0	8.1	5.8	2.5	3.4
[Pt(A)(^{OH}L)]	8.6	1.3	12.3	2.9	2.7	0.9	7.6	1.1	19.8	0.8
[Pt(B)(^{OH}L)]OTf	9.6	10.1	9.4	3.5	3.1	14.1	10.2	20.1	24.0	14.7
[Pt(A)(^{OH}L^{OH})]	1.8	7.5	2.2	4.9	1.0	1.5	1.8	1.8	2.9	1.2
[Pt(B)(^{OH}L^{OH})]OTf	8.6	6.4	6.3	5.4	2.4	3.1	10.4	4.0	22.6	2.4
[Pt(A)(^{P}L)]	9.1	1.5	12.5	1.5	2.3	0.6	9.2	1.0	19.6	0.7
[Pt(B)(^{P}L)]OTf	9.3	3.1	6.4	1.7	2.7	7.2	10	15.1	22.4	6.8
[Pt(A)(^{P}L^{P})]	4.3	1.6	3.3	1.9	1.4	0.8	4.2	1.1	8.4	0.8
[Pt(B)(^{P}L^{P})]OTf	6.3	3.2	8.8	2.8	2.6	1.6	9.6	1.8	20.3	1.3

0 1 25

[a] Change in luminescence determined as the ratio of the emission in the presence of 12 equiv. of oligonucleotide and the emission in the absence of oligonucleotide. [b] Determined at 400 nm. [c] Determined at 500 nm (complexes with monofunctionalized ligand) and 525 nm (complexes with difunctionalized ligand), respectively.

ns range was measured for the luminescence at *ca.* 400 nm (emission from the singlet manifold), whereas the lifetime of the emission at *ca.* 510 nm was in the μs range (stemming from the lowest triplet state). Based on these results, it can be concluded that the emission at *ca.* 400 nm is due to fluorescence, whereas phosphorescence occurs at wavelengths >500 nm. It is noteworthy that no lifetimes could be measured for the ligand precursor, indicating that the ligand precursor is *not* responsible for the fluorescence of the difunctionalized complexes. It is also interesting to note that the phosphorescence lifetime of [Pt(A)(^{M}L)] increases about threefold in the presence of *bcl2*-mid (Table 5), clearly indicating an interaction between metal complex and DNA.

CD spectroscopy

CD spectroscopy was used to study the conformation of the four G-DNA quadruplexes (*c-myc22*, *bcl2*-mid, *c-kit*, and H-telo) and the double-stranded DNA (ds26), and to investigate conformational changes in the presence of the Pt(II) complexes. In most cases, changes in the CD spectrum were found to be within experimental uncertainty (see ESI, Fig. S50–S65†). For *c-myc22*, H-telo, and ds26, no relevant changes are observed in the CD spectra upon addition of most of the complexes. In contrast, statistically relevant differences are found when adding some of the complexes to *bcl2*-mid, and to a lesser extent to *c-kit*. It should be noted that the absence of any change in the CD spectra does not necessarily rule out an interaction of DNA and metal complex. Likewise, CD-spectroscopic changes do not need to indicate structural changes, they may also arise from the formation of a new chromophore upon DNA/complex interaction. Table 6 presents a general overview of how the addition of the respective metal complexes influences the molar ellipticity in the CD spectra of the DNA. Clearly, *bcl2*-mid and *c-kit* are the quadruplexes whose CD spectra are most affected by the Pt(II) complexes. Two selected examples will be discussed in the following.

Fig. 5a shows the CD spectrum of *c-myc22* in the presence of increasing amounts of [Pt(B)(^{M}L)]OTf, *i.e.*, the only complex significantly influencing the CD spectrum of *c-myc22*. The spectra display a gradual decrease of the positive Cotton effect at 266 nm in the presence of the complex, clearly indicating an interaction between complex and DNA. Similarly, [Pt(B)(^{P}L^{P})]OTf affects *bcl2*-mid (Fig. 5b). Here, a complete flattening of the signal is observed, indicating an unfolding of the quadruplex in the presence of the complex. The minor peak appearing at *ca.* 358 nm is outside the wavelength region of G4-based

Table 5 Overview of photoluminescence lifetimes (τ)[a]

Compound	$\tau_{(Ar)}$ (ns) @ *ca.* 400 nm	$\tau_{(Ar)}$ (μs) @ *ca.* 510 nm
^{Cl}LH^{Cl}	n.d.[b]	n.d.[b]
[Pt(A)(^{Cl}L^{Cl})]	10.76 ± 0.07[c] [13.82 ± 0.05 (93%), 2.9 ± 0.1 (7%)]	2.02 ± 0.01[d] [3.55 ± 0.04 (88%), 0.50 ± 0.01 (12%)]
[Pt(A)(^{M}L)]	n.d.[b]	1.37 ± 0.03[e]
bcl2-mid·[Pt(A)(^{M}L)]	4.71 ± 0.04[f] [12.37 ± 0.09 (63%), 2.29 ± 0.02 (37%)]	3.82 ± 0.01[e] [6.20 ± 0.04 (74%), 1.84 ± 0.02 (26%)]

[a] Conditions: Ar atmosphere, 10 μM solution, λ_{exc} = 340 nm. [b] Value could not be determined due to the weak signal. [c] λ_{em} = 410 nm. [d] λ_{em} = 520 nm. [e] λ_{em} = 510 nm. [f] λ_{em} = 415 nm. Amplitude-weighted average lifetimes are indicated along with the individual components in square brackets and their relative amplitudes in parentheses. The corresponding original data, together with the fitting parameters, are given in the ESI (Fig. S45–S49).†

Table 6 Heatmap illustrating percentaged change of selected molar ellipticity maxima of the investigated oligonucleotide sequences after addition of the complexes (5 equiv.)[a]

Complex	*c-myc*22 266 nm	*bcl2*-mid 266 nm	*bcl2*-mid 290 nm	*c-kit* 242 nm	*c-kit* 263 nm	H-telo 295 nm	ds26 280 nm
[Pt(A)(^{Cl}L)]				38			
[Pt(B)(^{Cl}L)]OTf				−32			
[Pt(A)(^{Cl}L^{Cl})]		33					
[Pt(B)(^{Cl}L^{Cl})]OTf							−30
[Pt(A)(^{M}L)]				50			
[Pt(B)(^{M}L)]OTf	−38	−57					
[Pt(A)(^{M}L^{M})]							
[Pt(B)(^{M}L^{M})]OTf							
[Pt(A)(^{OH}L)]		31					
[Pt(B)(^{OH}L)]OTf		−36					
[Pt(A)(^{OH}L^{OH})]		68		54	30		
[Pt(B)(^{OH}L^{OH})]OTf					30		
[Pt(A)(^{P}L)]		37		42			
[Pt(B)(^{P}L)]OTf							
[Pt(A)(^{P}L^{P})]							
[Pt(B)(^{P}L^{P})]OTf		−99	−44	−37		−33	

−100 −50 0 50 100

[a] Only changes with absolute values exceeding 30% are shown to exclude irrelevant changes in rather noisy regions of the spectrum.

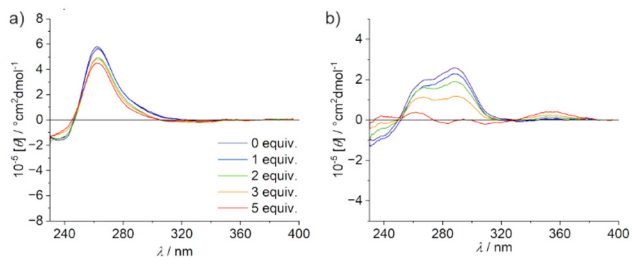

Fig. 5 CD spectra of (a) *c-myc22* upon stepwise addition of [Pt(B)(^{M}L)]OTf and (b) *bcl2*-mid upon stepwise addition of [Pt(B)(^{P}L^{P})]OTf (0–5 equiv.). Conditions: DNA (3 μM), LiCl (90 mM), KCl (10 mM), MOPS (5 mM, pH 7.4), 20 °C.

peaks.[63] It is likely an induced circular dichroism due to an interaction of the metal complex with the unfolded (yet chiral) oligonucleotide. Interestingly, this appears to be the only combination of G4 DNA and Pt(II) complex is this study where such an effect is observed (see ESI, Fig. S50–S65†).

Table 6 indicates that an increase in molar ellipticity upon the addition of a complex is observed almost exclusively for complexes bearing auxiliary ligand A. In contrast, interactions with complexes containing auxiliary ligand B mostly lead to decreasing molar ellipticities, indicating either less neatly stacked tetrads or the onset of an unfolding process.

FRET

Due to the changes in the photophysical properties of the Pt(II) complexes in the presence of *bcl2*-mid as well as its significant structural changes in the presence of selected complexes (as evident from the CD spectra, *vide supra*), the thermal stability of *bcl2*-mid was evaluated experimentally. Temperature-dependent Förster resonance energy transfer (FRET) measurements were therefore carried out using a suitably modified *bcl2*-mid sequence (*i.e.*, with terminally appended carboxyfluorescein (FAM) and DABCYL moieties).[64] However, the CD spectrum of FAM-*bcl2*-mid-DABCYL differs significantly from that of unmodified *blc2*-mid. Instead of adopting a hybrid topology, the labelled sequence folds into a parallel quadruplex structure, as the close resemblance of its CD spectrum with that of *c-myc*22 shows (Fig. S66†). Such a parallel fold is known as one possible structure of native *bcl2*.[65] Hence, even though the results of the FRET melt assay cannot be directly correlated with the other data collected for *bcl2*-mid in this study, they are of potential biological relevance, as they exemplify the interaction of the Pt(II) complexes with a parallel quadruplex structure. Reference measurements in the absence of DNA confirmed that no fluorescence interference arises from the compounds themselves when excited under identical conditions (data not shown). Luminescence spectra were recorded in the absence and presence of five equiv. of the respective metal complex. In most cases, the addition of the metal complex does not influence the melting temperature T_m of FAM-*bcl2*-mid-DABCYL, with T_m amounting to 62 °C both in the absence and the presence of the metal complex. Amongst the complexes bearing auxiliary ligand B, only those with a phosphate ester or a hydroxy group lead to an increase in T_m. In addition, the melting temperature in the presence of the monofunctionalized complexes [Pt(B)(^{P}L)]OTf and [Pt(B)(^{OH}L)]OTf increases to a larger extent compared to the respective difunctionalized complexes. For example, T_m increases from an initial 62 °C by 8.8 °C to 70.8 °C (Fig. 6a) upon the addition of 5 equiv. of [Pt(B)(^{P}L)]OTf. With [Pt(B)(^{OH}L)]OTf, the largest increase in melting temperature of any of the monofunctionalized complexes was observed, namely by 15.1 °C to 77.1 °C. The corres-

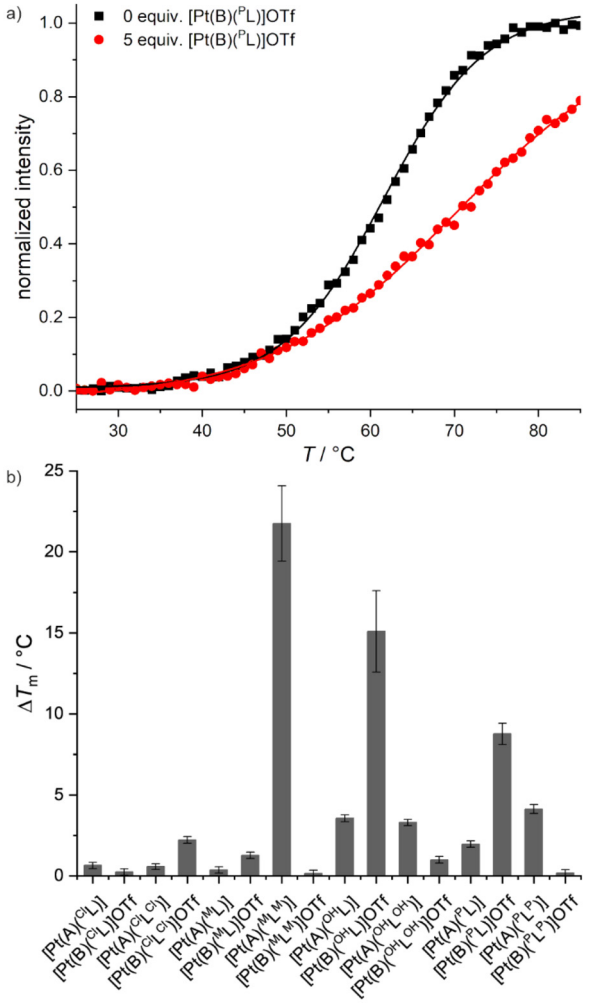

Fig. 6 (a) Melting curves of FAM-*bcl2*-mid-DABCYL in the absence (black) and presence (red) of 5 equiv. of [Pt(B)(^{P}L)]OTf; (b) melting point increase (ΔT_m) of FAM-*bcl2*-mid-DABCYL upon the addition of 5 equiv. of the respective metal complexes. Conditions: DNA (0.2 μM), LiCl (95 mM), KCl (5 mM), MOPS (5 mM, pH 7.4), λ_{exc} = 490 nm, λ_{em} = 520 nm.

ponding difunctionalized complexes induce no significant melting point increase ([Pt(B)(^{P}L^{P})]OTf) and a minor increase of only 1.0 °C ([Pt(B)(^{OH}L^{OH})]OTf), respectively. Among the difunctionalized complexes, [Pt(A)(^{P}L^{P})] and [Pt(A)(^{M}L^{M})] show the largest increase in T_m, with a ΔT_m of 4.1 °C and 21.8 °C, respectively. Fig. 6b shows the change in T_m on the addition of the metal complexes. A compilation of all melting curves can be found in the ESI (Fig. S67–S74).†

Interestingly, no obvious correlation exists between the stabilizing effect of a metal complex and its influence on the CD spectrum of G4 DNA. For example, [Pt(A)(^{M}L^{M})] exerts the highest stabilizing effect on G4 DNA (Fig. 6b) but does not seem to influence their topology at all (Table 6). Similarly, [Pt(B)(^{P}L^{P})]OTf strongly influences the CD spectrum of *bcl2*-mid (Fig. 5b), but its presence does not lead to a change of the melting temperature of this G4 DNA (see ESI, Fig. S74†). It can therefore be concluded that both, structural changes and thermal G4 DNA stabilization, should be considered independent indicators for an interaction between DNA and metal complex.

Cryo-ESI-MS

To gain further information on the interaction capacity and adduct formation ability between the Pt(II) complexes and guanine quadruplex oligonucleotide sequences, their mixtures were examined by cryo-electrospray ionization mass spectrometry (cryo-ESI-MS). This technique also enables an estimation of the stoichiometry between the bound complexes and the respective folded secondary structures. The ultra-mild ionization conditions were chosen to be able to detect weak non-covalent interactions and to improve the signal-to-noise ratio. Due to limitations elicited by the experimental conditions, *i.e.*, the use of solutions of KCl, LiCl, and the volatile triethylammonium acetate (pH 7.0) in a mixture of water and acetonitrile (1 : 1, v/v), only complexes bearing the auxiliary ligand B could be analysed, as all other complexes are poorly soluble in water or acetonitrile at the concentrations required to prepare the stock solutions. Using the combination of *c-myc22* and [Pt(B)(^{M}L)]OTf as an example, a general trend of binding affinity and binding stoichiometry was established. At a ratio of 1 : 1 (DNA : complex), barely any signal is detectable that could be assigned to an adduct of DNA and complex. When the amount of DNA is doubled (giving a 2 : 1 ratio), a 1 : 1 adduct of DNA and complex can clearly be observed. Likewise, in the presence of excess complex (1 : 2 ratio), both 1 : 1 and 1 : 2 adducts are present. It can therefore be concluded that both 1 : 1 and 1 : 2 binding stoichiometries are possible. Moreover, the 1 : 1 adduct appears to be more stable than the 1 : 2 adduct (Fig. 7).[66]

In all possible combinations of DNA and complex (or, as a reference measurement, of DNA and ligand precursor), a binding stoichiometry of 1 : 3 was never detected (data not shown), indicating a scarcity of binding sites on the DNA. Likewise, sandwich-type adducts of a 2 : 1 stoichiometry (DNA : complex) were not detected in any of the measurements (data not shown). In summary, the cryo-ESI-MS data confirm that an interaction of the complexes with DNA is possible. On the other hand, the fact that adducts of different stoichiometry are present simultaneously prevents a meaningful estimation of binding constants based on the data obtained in the spectroscopic titration experiments.

Unfortunately, additional experiments to quantify the affinity of the complexes and G4 DNA by means of isothermal titration calorimetry (ITC) or by thiazole orange (TO) displacement assay failed to produce meaningful data. In case of ITC, solubility issues negatively influenced the measurements. In addition, all complexes with auxiliary ligand A are only poorly soluble in water. The high concentrations required for the ITC titrations could only be achieved in DMSO. Here, the large heat of dilution of this solvent prevented any meaningful measurement (data not shown). Likewise, the heat involved with the reaction of the complexes with auxiliary ligand B (which could

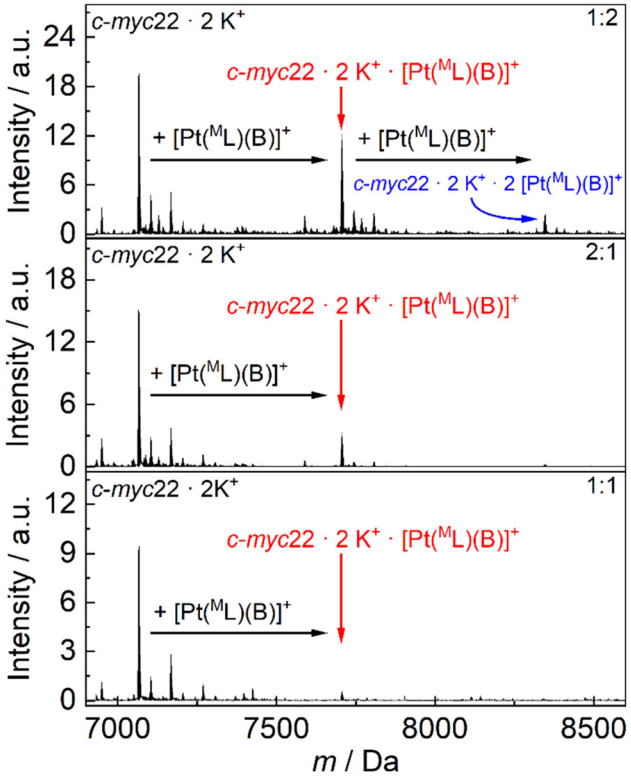

Fig. 7 Deconvoluted cryo-ESI-MS spectra of *c-myc22* and [Pt(B)(^{M}L)]OTf in DNA : complex ratios of 1 : 1 (bottom), 2 : 1 (middle) and 1 : 2 (top).

be provided as an aqueous solution) was too small in the applied concentration range, so that the titration data could not be fitted (data not shown). Based on the concentrations used in the experiments (150 μM *bcl2*-mid, 750 μM metal complex), a very rough estimation places the binding constant K_a in the range of 10^2 M^{-1} to 10^3 M^{-1}, *i.e.*, relatively low.[67]

In the fluorescent intercalator displacement assay, the displacement of TO from the DNA (as monitored by an increase in fluorescence at 540 nm) upon the addition of increasing amounts of the respective metal complex can be used to quantify the relative affinities of TO and metal complex to the DNA.[68] Using this assay, all complexes show a rather low affinity towards G4 DNA compared to thiazole orange (see ESI, Fig. S75–S82†). In fact, most complexes do not even displace half of TO from the DNA at a complex concentration of 30 μM. A comparison with the porphyrin-derived tetracationic G4 binder TMPyP4, of which only 0.106 μM are required to achieve this effect,[68] indicates the low affinity of the complexes.

Experimental and computational details

Materials and methods

Reagents. Chemicals were purchased from ABCR, Acros Organics, Fisher Scientific, VWR, Alfa Aesar, Merck, and Glen Research and were used without prior purification unless mentioned otherwise. The labelled oligonucleotide, 5′-FAM-d(GGG CGC GGG AGG AAT TGG GCG GG)-DABCYL-3′, was purchased from Eurogentec. Unlabelled oligonucleotides were synthesized, purified, and characterized as reported previously.[69] The following oligonucleotides were investigated: *c-myc22*, d(TGA GGG TGG GTA GGG TGG GTA A); *bcl2*-mid, d(GGG CGC GGG AGG AAT TGG GCG GG); *c-kit*, d(AGG GAG GGC GCT GGG AGG AGG G), H-telo, d(AGG GTT AGG GTT AGG GTT AGG G); ds26, d(CAA TCG GAT CGA ATT CGA TCC GAT TG). HPLC chromatograms confirming the purity of the oligonucleotides can be found in the ESI (Fig. S83–S87).†

Anhydrous solvents were distilled, dried, and stored following standard protocols. Silica gel column chromatography was carried out by using Silica-60, having a particle size of 40–63 μm, obtained from VWR. A particle size of 63–200 μm was used for column chromatography with aluminium oxide (MP Alumina N – Super I, neutral pH) from MP Biomedicals. Silver phenylacetylide,[70] 2-ethynyl-6-phenylpyridine (**1**),[36] 2-(1-(3-bromopropyl)-1*H*-1,2,3-triazol-4-yl)-6-phenylpyridine (**2**),[71] 4-(6-bromopyridin-2-yl)phenol (**3**),[72] ^{M}LH,[71] ^{OH}LH,[36] [PtCl(^{OH}L)],[73] trimethylpropargylammonium hexafluorophosphate,[74] and trimethylpropargylammonium triflate[74] were synthesized according to literature methods. All other reagents were obtained commercially and used as supplied. All DNA solutions were heated to 85 °C for 5 min and then stored at 4 °C.

General instrumentation. Elemental analyses were performed on a UNICUBE instrument. NMR spectra were recorded at 300 K on Bruker Avance(I) 400, Bruker Avance(III) 400, Bruker Avance Neo 400, and Bruker Avance Neo 500 spectrometers. In the case of $CDCl_3$, tetramethylsilane (TMS, δ_H = 0 ppm) was used as an internal standard. When using D_2O, sodium trimethylsilylpropionate (TSP) was used as an internal standard. In the case of MeOD-d_4, CD_2Cl_2, DMF-d_7 and DMSO-d_6, chemical shifts were referenced to residual methanol-d_3 (δ_H = 3.31 ppm), dichloromethane-d_1 (δ_H = 5.32 ppm), DMF-d_6 (δ_H = 8.02 ppm), and DMSO-d_5 (δ_H = 2.50 ppm), respectively. $^{15}N\{^1H\}$ NMR spectra were referenced to liquid ammonia, $^{19}F\{^1H\}$ NMR spectra to CCl_3F, $^{31}P\{^1H\}$ NMR spectra to phosphoric acid (85%), and $^{195}Pt\{^1H\}$ NMR spectra to a solution of Na_2PtCl_6 (1.2 M) in D_2O. For the assignment of NMR resonances, please see structural representations given in the ESI.† The pH values of the aqueous solutions were measured using an inoLab 720 pH meter from WTW (microelectrode: Blueline 16 pH from Schott). pD values were obtained by adding 0.4 to the pH meter reading.[75]

Mass spectrometry. ESI mass spectra were recorded in the Organic Chemistry Institute on an LTQ Orbitrap XL from Thermo Fisher Scientific or in the Institute of Inorganic and Analytical Chemistry on an Impact II from Bruker. For the cryo-ESI-MS measurements, the sample was applied to the Impact II using an injection syringe and a flow rate of 3.5 μL min^{-1}. The temperature of the dry gas was 30 °C and the spray gas set to 10 °C. In addition to the pressure of 0.06 MPa and the capillary voltage of 2600 V as well as the end plate offset of

350 V, the range to be scanned was 150–3000 *m*/*z*. Sodium formate clusters were used for calibration. A mixture of acetonitrile and water (1 : 1, v/v) consisting of DNA (30 μM), KCl (1 μM), and tetraethylammonium acetate (50 μM, pH 7.0) was used for the measurements. The data were processed according to the deconvolution algorithm "Maximum Entropy".[76]

UV/Vis spectroscopy. The UV/vis spectra were recorded on an Agilent Cary Bio 100 spectrometer in a quartz cuvette with a path length of 1 cm. In case of the metal complexes, the spectrum was measured at 20 °C from 200–800 nm in doubly distilled water at a scan rate of 400 nm min^{-1} at concentrations of 3 μM. All spectra were recorded in triplicate with a data interval of 1 nm.

Photoluminescence spectroscopy. The fluorescence enhancement studies were carried out on a Jasco FP-8300 fluorometer. The hybridized G4 DNA was added to a solution of metal complex (1 μM), LiCl (90 mM), KCl (10 mM), and MOPS (5 mM, pH 7.4). Emission spectra were recorded with an excitation wavelength λ_{exc} of 320 nm, a temperature of 20 °C and in a range from 300–750 nm. The scan rate was set to 500 nm min^{-1} and the measurements were accumulated three times with a data interval of 0.5 nm and an excitation and emission bandwidth of 5 nm each. The same device parameters were selected when recording excitation spectra at an emission wavelength of 500 nm.

Photoluminescence lifetimes were recorded in TCSPC mode with a PicoHarp 300 with a minimum base resolution of 4 ps or in MCS mode with a TimeHarp 260. Emission and excitation spectra were corrected for the intensity of the radiation source (lamp and grating) using standard correction functions. The analysis of the lifetimes of the excited states were performed with the commercially available EasyTau 2 software from PicoQuant. The quality of the data fit was ensured by minimizing the reduced chi-square function (χ^2) and by manually checking the weighted residuals and their autocorrelation. Solvents used were of spectrometric quality (Uvasol®, Merck).

Photoluminescence quantum yields were measured with a Hamamatsu Photonics absolute PL quantum yield measurement system (C9920-02) equipped with a L9799-01 CW Xe light source (150 W), a monochromator, a C7473 photonic multichannel analyser, an integrating sphere and employing U6039-05 software (Hamamatsu Photonics, Ltd, Shizuoka, Japan).

Fluorescence intercalator displacement studies. Thiazole orange (TO) was purchased from Sigma Aldrich. A solution of G4 DNA (0.25 μM), TO (0.5 μM for G4 DNA and 0.75 μM for dsDNA), LiCl (90 mM), KCl (10 mM), and MOPS (5 mM, pH 7.4) was used for the displacement studies. The influence of increasing concentrations (0–30 μM) of metal complexes on the fluorescence emission of TO was investigated. After each addition, there was a 3 min incubation time prior to the measurement. The emission spectrum was recorded from 200–750 nm with a data interval of 0.5 nm and a scan rate of 500 nm min^{-1} at an excitation wavelength of 501 nm. Data were accumulated threefold, applying an excitation and emission bandwidth of 5 nm each and a temperature of 20 °C.

Isothermal titration calorimetry. For isothermal titration calorimetry, *bcl2*-mid and the respective complex were dissolved in MilliQ water and DMSO. Measurements were carried out with a TA Instrument Nano ITC Low Volume with a cell volume of 170 μL using ITCRun version 2.1.7.0, firmware version 1.31. All titrations were performed with a 50 μL syringe in 20 injections of 2.5 μL each at a temperature of 25 °C and with a stirring speed of 350 rpm. The Pt(II) complex (750 μM) was added to *bcl2*-mid (150 μM) in MOPS (5 mM, pH 7.4), KCl (10 mM), and LiCl (90 mM).

CD spectroscopy. The CD spectra of the investigated oligonucleotides were recorded at 20 °C in a wavelength range of 230–400 nm with increasing amounts of the metal complex in a quartz cuvette with a path length of 1 cm and three-fold accumulation. The spectra were recorded on a Jasco J-815 CD spectrometer with a scan rate of 200 nm min^{-1} and a data interval of 0.1 nm. A solution of DNA (3 μM), KCl (10 mM), LiCl (90 mM), and MOPS (5 mM, pH 7.4) was used. For the metal complexes, a stock solution (750 μM) in DMSO or MilliQ water was used. For all spectra, a manual baseline correction was applied, followed by a smoothing algorithm using a Savitzky–Golay filter with 100 points. The spectra shown in Fig. 5 were recorded with 30-fold accumulation, and a different smoothing algorithm was applied (moving average, 150 points).

FRET-based DNA melting studies. For the FRET-based melting studies, a solution of DNA (0.2 μM), MOPS buffer (5 mM, pH 7.4), LiCl (95 mM), and KCl (5 mM) was used. The data were recorded on a Chirascan V100 spectrometer from Applied Photophysics with an additional fluorescence detector, Chirascan CCD fluorometer. In a quartz cuvette of 1 cm thickness, the melting curves were recorded from 25–85 °C with an interval of 1 °C. The emission spectrum was recorded after excitation at 490 nm. The integration time was 1000 ms, the average scan accumulation 30, the excitation and emission bandwidths 5 nm. The normalized emission at 525 nm was plotted against temperature. The FRET melting curves were determined in the presence of 0 and 5 equivalents of the metal complexes, respectively. Data points were fitted using the dose–response model function. T_m was determined by the inflection point of the dose–response model function. The error of ΔT_m was calculated by using Gaussian error propagation.

Crystallography. Crystals suitable for X-ray crystallography were obtained as described in the Experimental section. Intensity data were collected with monochromated MoKα radiation on a Bruker D8-Venture diffractometer with Photon III detector using the APEX4 software suite.[77] The collection method involved ω scans. Data reduction was carried out using the program SAINT.[78] The crystal structures were solved by Intrinsic Phasing using SHELXT.[79] Non-hydrogen atoms were first refined isotropically followed by anisotropic refinement by full matrix least-squares calculation based on F^2 using SHELXL.[80] H atoms were positioned geometrically and allowed to ride on their respective parent atoms. Complex [Pt(A)(^{Cl}L)] crystallized with one molecule of CH_2Cl_2, complex

[PtCl($^{OH}L^{OH}$)] with half a molecule of DMF per unit cell, which was disordered across the inversion centre. Additionally, one OH group of [PtCl($^{OH}L^{OH}$)] was rotationally disordered and refined in two positions (0.6 : 0.4). Molecular graphics were created using the program ORTEP-3 for Windows.[81,82]

Computational details. DFT calculations were performed using Gaussian 16 on the PALMA II computing cluster at the University of Münster.[83] The PBE0 hybrid exchange–correlation functional[84] was used to calculate the molecular volume and optimize the S_0 state, and the SDD basis set[85,86] was used to calculate the Kohn–Sham molecular orbitals. Solvent effects of water were taken into account by the polarizable continuum model (PCM) within an integral equation formalism.[87] Dispersive interactions were included in the calculations by the D3 version of Grimme's dispersion with Becke–Johnson damping.[88,89] To further calculate the charge-balance parameter ν and the molecular polarity index MPI, the data from the DFT calculations were interpreted by multifunctional wave function analysis (MultiWFN).[57]

Synthetic procedures

General procedure for the click reaction. The azide (2.0 equiv.) and the alkyne (1.0 equiv.) were dissolved in isopropanol (2 mL mmol^{-1} alkyne), tetrahydrofuran (8 mL mmol^{-1} alkyne), and water (2 mL mmol^{-1} alkyne). $CuSO_4{\cdot}5\ H_2O$ (20 mol%) and sodium ascorbate (0.5 equiv.) were then added to the reaction mixture. The mixture was stirred at room temperature overnight. Dichloromethane and a saturated aqueous solution of EDTA were then added. The aqueous phase was extracted three times with dichloromethane. The combined organic phases were dried ($MgSO_4$), the solvent was removed under reduced pressure, and the crude product was purified by column chromatography.

General procedure for the synthesis of complexes with auxiliary ligand A. Silver phenylacetylide (3.0 equiv.) and the chlorido complex (1.0 equiv.) were added to a dry round bottom flask together with anhydrous triethylamine (10 mL mmol^{-1} complex) and anhydrous DMF (90 mL mmol^{-1} complex). The round bottom flask was wrapped with aluminium foil. The solution was stirred overnight at 75 °C and the solvent was removed *in vacuo*. The crude product was purified by column chromatography.

General procedure for the synthesis of complexes with auxiliary ligand B. The alkyne (2.5 equiv.) and the chlorido complex (1.0 equiv.) were added together in anhydrous triethylamine (4 mL mmol^{-1} complex) and anhydrous DMF (10 mL mmol^{-1} complex) in a round bottom flask. Copper iodide (8 mol%) was added and the mixture was stirred overnight. The resulting solid was washed with ethanol and diethyl ether. The product was then dried *in vacuo*.

Synthesis of ^{P}LH. Diethyl (2-bromoethyl)phosphonate (490 mg, 2.00 mmol, 2.0 equiv.) and NaN_3 (195 mg, 3.00 mmol, 3.0 equiv.) were dissolved in dry acetone (10 mL). The reaction mixture was heated to reflux overnight, then filtered, and the residue was washed with acetone. The solvent was removed at reduced pressure. The general procedure for the click reaction was applied to the resulting azide and compound **1** (179 mg, 1.00 mmol), and the crude product was purified by column chromatography (SiO_2, ethyl acetate). The product was obtained as a colourless oil. Yield: 48% (185 mg, 0.479 mmol). ^{1}H NMR (400 MHz, $CDCl_3$): δ (ppm) = 8.33 (s, 1H, H-15), 8.11 (d, J = 7.7 Hz, 1H, H-8), 8.05 (d, J = 7.5 Hz, 2H, H-3), 7.83 (t, J = 7.8 Hz, 1H, H-9), 7.67 (d, J = 7.8 Hz, 1H, H-10), 7.52–7.38 (m, 3H, H-1, H-2), 4.77–4.63 (m, 2H, H-16), 4.19–4.03 (m, 4H, H-19), 2.55–2.42 (m, 2H, H-17), 1.32 (t, J = 7.1 Hz, 6H, H-20). ^{13}C{^{1}H} NMR (101 MHz, $CDCl_3$): δ (ppm) = 156.9 (C-5), 149.9 (C-7), 148.8 (C-11), 139.0 (C-4), 137.6 (C-9), 129.1 (C-1), 128.7 (C-2), 126.9 (C-3), 122.7 (C-15), 119.5 (C-10), 118.4 (C-8), 62.2 (d, $^2J_{C,P}$ = 6.5 Hz, C-19), 44.7 (d, $^2J_{C,P}$ = 1.8 Hz, C-16), 27.4 (d, $^1J_{C,P}$ = 141 Hz, C-17), 16.4 (d, $^3J_{C,P}$ = 6.0 Hz, C-20). ^{15}N{^{1}H} NMR (41 MHz, $CDCl_3$): δ (ppm) = 362 (N-13), 348 (N-12), 297 (N-6), 247 (N-14). ^{31}P{^{1}H} NMR (162 MHz, $CDCl_3$): δ (ppm) = 25.4 (P-18). HRMS (m/z) [$C_{19}H_{23}N_4O_3P$ + H]$^+$: calcd: 387.1581, found: 387.157. Elem. Anal. for $C_{19}H_{23}N_4O_3P$ (%) calcd: C 59.1, H 6.0, N 14.5, found: C 58.8, H 6.1, N 14.4.

Synthesis of ^{Cl}LH. A solution of ^{OH}LH (164 mg, 0.585 mmol, 1.0 equiv.) in dry CH_2Cl_2 (8 mL) was cooled to 0 °C, then thionyl chloride (170 µL, 2.34 mmol, 4.0 equiv.) was added dropwise. The mixture was stirred overnight at room temperature. After careful addition of water (10 mL), the crude product was extracted with CH_2Cl_2. The organic layer was dried ($MgSO_4$) and evaporated to dryness. The crude product was purified by column chromatography (cyclohexane : ethyl acetate, 8 : 2). The product was obtained as white solid. Yield: 87% (152 mg, 0.510 mmol). ^{1}H NMR (400 MHz, $CDCl_3$): δ (ppm) = 8.29 (s, 1H, H-15), 8.12 (d, J = 7.8 Hz, 1H, H-8), 8.10–8.03 (m, 2H, H-3), 7.84 (t, J = 7.8 Hz, 1H, H-9), 7.68 (d, J = 7.9 Hz, 1H, H-10), 7.53–7.46 (m, 2H, H-2), 7.45–7.40 (m, 1H, H-1), 4.62 (t, J = 6.6 Hz, 2H, H-16), 3.57 (t, J = 6.1 Hz, 2H, H-18), 2.49–2.40 (m, 2H, H-17). ^{13}C{^{1}H} NMR (101 MHz, $CDCl_3$): δ (ppm) = 156.9 (C-5), 150.0 (C-7), 148.8 (C-11), 139.1 (C-4), 137.6 (C-9), 129.1 (C-1), 128.7 (C-2), 126.9 (C-3), 122.8 (C-15), 119.5 (C-10), 118.4 (C-8), 47.2 (C-16), 41.1 (C-18), 32.6 (C-17). ^{15}N{^{1}H} NMR (41 MHz, $CDCl_3$): δ (ppm) = 363 (N-13), 348 (N-12), 298 (N-6), 246 (N-14). HRMS (m/z) [$C_{16}H_{15}N_4Cl$ + Na]$^+$: calcd: 321.0877, found: 321.0881. Elem. Anal. for $C_{16}H_{15}N_4Cl$ (%) calcd: C 64.3, H 5.1, N 18.8, found: C 64.3, H 5.1, N 18.8.

Synthesis of 4-(6-ethynylpyridin-2-yl)phenol (3). A solution of compound **2** (3.00 g, 12.0 mmol, 1.0 equiv.) and trimethylsilyl acetylene (5.12 mL, 36.0 mmol, 3.0 equiv.) in a mixture of triethylamine (40 mL) and THF (40 mL) was purged with argon for 30 min. Subsequently, CuI (228 mg, 1.20 mmol, 0.1 equiv.) and [$PdCl_2(PPh_3)_2$] (421 mg, 0.600 mmol, 5 mol%) were added under argon atmosphere, and the mixture was stirred at 80 °C overnight. It was then cooled to 0 °C, neutralized with aqueous HCl (6 M, 100 mL) and extracted three times with CH_2Cl_2. The combined organic layers were dried ($MgSO_4$), the solvent removed *in vacuo*, and the residue filtered over Celite® and silica gel using diethyl ether. Finally, the solvent was removed *in vacuo*. The crude product was dissolved in a mixture of tetrahydrofuran (20 mL) and methanol (20 mL) and mixed with an

aqueous NaOH solution (20 mL, 1 M). The mixture was stirred for 1 h at room temperature. The solvent was removed under reduced pressure. Water was added to the residue, and the product was extracted with CH_2Cl_2, the solution was dried ($MgSO_4$) and evaporated to dryness. The crude product was purified by column chromatography (SiO_2, cyclohexane : ethyl acetate, 8 : 2), and the product was obtained as a yellow solid. Yield: 64% (1.49 g, 7.65 mmol). ^{1}H NMR (400 MHz, DMSO-d_6): δ (ppm) = 9.84 (s, 1H, H-1), 7.95–7.88 (m, 2H, H-4), 7.87–7.77 (m, 2H, H-10, H-11), 7.41 (dd, J = 7.1, 1.4 Hz, 1H, H-9), 6.90–6.84 (m, 2H, H-3), 4.30 (s, 1H, H-13). ^{13}C{^{1}H} NMR (101 MHz, DMSO-d_6): δ (ppm) = 158.9 (C-2), 156.5 (C-6), 141.2 (C-8), 137.5 (C-10), 128.6 (C-5), 128.0 (C-4), 124.8 (C-9), 119.1 (C-11), 115.5 (C-3), 83.4 (C-12), 79.6 (C-13). HRMS (m/z) $[C_{13}H_9NO + H]^+$: calcd: 196.0757, found: 196.0757. Elem. Anal. for $C_{13}H_9NO$ (%) calcd: C 80.0, H 4.7, N 7.2, found: C 79.9, H 4.7, N 7.0.

Synthesis of diethyl (2-(4-(6-(4-hydroxyphenyl)pyridin-2-yl)-1*H*-1,2,3-triazol-1-yl)ethyl)phosphonate (4). A solution of diethyl (2-bromoethyl)phosphonate (908 µL, 5.00 mmol, 1.6 equiv.) and NaN_3 (488 mg, 7.51 mmol, 2.4 equiv.) in acetone (10 mL) was heated to reflux overnight, filtered, and the precipitate washed with acetone. The solvent was removed under reduced pressure. The resulting azide was reacted with compound **3** (600 mg, 3.07 mmol, 1.0 equiv.) according to the general procedure for the click reaction, and the crude product was purified by column chromatography (SiO_2, ethyl acetate). The product was obtained as a beige solid. Yield: 35% (421 mg, 1.05 mmol). ^{1}H NMR (400 MHz, CD_2Cl_2): δ (ppm) = 8.40 (s, 1H, H-1), 8.34 (s, 1H, H-16), 8.01–7.92 (m, 3H, H-9, H-4), 7.77 (t, J = 7.8 Hz, 1H, H-10), 7.59 (d, J = 7.9 Hz, 1H, H-11), 7.04–6.94 (m, 2H, H-3), 4.72 (t, J = 7.6 Hz, 2H, H-17), 4.18–4.06 (m, 2H, H-20), 2.52 (t, J = 7.6 Hz, 2H, H-18), 1.31 (t, J = 7.1 Hz, 5H, H-21). ^{13}C{^{1}H} NMR (101 MHz, CD_2Cl_2): δ (ppm) = 158.7 (C-2), 157.1 (C-6), 150.1 (C-8), 149.2 (C-12), 137.9 (C-10), 131.1 (C-5), 128.6 (C-4), 123.3 (C-16), 118.9 (C-11), 117.7 (C-9), 116.0 (C-3), 63.0 (d, $^3J_{C,P}$ = 6.6 Hz, C-20), 45.0 (d, $^2J_{C,P}$ = 1.9 Hz, H-17), 27.5 (d, $^1J_{C,P}$ = 141.4 Hz, C-18), 16.6 (d, $^3J_{C,P}$ = 6.1 Hz, C-21). ^{15}N{^{1}H} NMR (41 MHz, CD_2Cl_2): δ (ppm) = 362 (N-14), 347 (N-13), 296 (N-7), 247 (N-15). ^{31}P{^{1}H} NMR (162 MHz, CD_2Cl_2): δ (ppm) = 26.1 (P-19). HRMS (m/z) $[C_{19}H_{23}N_4O_4P + H]^+$: calcd: 403.1530, found: 403.1530. Elem. Anal. for $C_{19}H_{23}N_4O_4P$ (%) calcd: C 56.7, H 5.8, N 13.9, found: C 56.8, H 5.8, N 13.7.

Synthesis of ^{P}LH^P. A solution of diethyl (hydroxymethyl) phosphonate (575 µL, 4.00 mmol, 2.7 equiv.) in CH_2Cl_2 (15 mL) and pyridine (393 µL) was cooled to −78 °C. Trifluoromethanesulfonic anhydride (780 µL, 4.60 mmol, 3.1 equiv.) was carefully added to the cooled solution. The mixture was stirred for 30 min at −78 °C and then for 1 h at room temperature. Subsequently, diethyl ether (50 mL) was added, filtered, and the combined organic layers were washed with aqueous HCl (1 M) and brine. The solvent was removed under reduced pressure and the intermediate product was used without further purification. Compound **4** (600 mg, 1.49 mmol, 1.0 equiv.), K_2CO_3 (415 mg, 3.00 mmol, 2.0 equiv.), and the crude product were dissolved in acetonitrile (30 mL) and heated to reflux overnight. The solvent was removed under reduced pressure and the crude product was purified by column chromatography (SiO_2, CH_2Cl_2 : CH_3OH, 100 : 3). The product was obtained as a brown oil. Yield: 61% (500 mg, 0.905 mmol). ^{1}H NMR (400 MHz, CD_2Cl_2): δ (ppm) = 8.33 (s, 1H, H-15), 8.11–8.05 (m, 2H, H-3), 8.02 (d, J = 7.7 Hz, 1H, H-8), 7.82 (t, J = 7.8 Hz, 1H, H-9), 7.65 (d, J = 7.9 Hz, 1H, H-10), 7.15–7.02 (m, 2H, H-2), 4.76–4.64 (m, 2H, H-16), 4.34 (d, $^2J_{H,P}$ = 10.1 Hz, 2H, H-21), 4.28–4.17 (m, 4H, H-23), 4.14–4.03 (m, 4H, H-19), 2.54–2.41 (m, 2H, H-17), 1.36 (t, J = 7.1 Hz, 6H, H-24), 1.30 (t, J = 7.1 Hz, 6H, H-20). ^{13}C{^{1}H} NMR (101 MHz, CD_2Cl_2): δ (ppm) = 160.1 (d, $^3J_{C,P}$ = 13.7 Hz, C-1), 156.6 (C-5), 150.4 (C-7), 149.1 (C-11), 138.0 (C-9), 133.2 (C-4), 128.6 (C-3), 123.1 (C-15), 119.1 (C-10), 118.2 (C-8), 115.0 (C-2), 63.3 (d, $^3J_{C,P}$ = 6.4 Hz, C-23), 62.7 (d, $^1J_{C,P}$ = 169.9 Hz, C-21), 62.6 (d, $^3J_{C,P}$ = 6.5 Hz, C-19), 45.1 ($^2J_{C,P}$ = 1.7 Hz, C-16), 27.6 (d, $^1J_{C,P}$ = 141.1 Hz, C-17), 16.7 (d, $^3J_{C,P}$ = 5.7 Hz, C-24), 16.6 (d, $^3J_{C,P}$ = 6.0 Hz, C-20). ^{15}N{^{1}H} NMR (41 MHz, CD_2Cl_2): δ (ppm) = 363 (N-13), 349 (N-12), 296 (N-6), 248 (N-14). ^{31}P{^{1}H} NMR (162 MHz, CD_2Cl_2): δ (ppm) = 25.4 (P-18), 18.7 (P-22). HRMS (m/z) $[C_{24}H_{34}N_4O_7P_2 + H]^+$: calcd: 553.1975, found: 553.1979. Elem. Anal. for $C_{24}H_{34}N_4O_7P_2$ (%) calcd: C 52.2, H 6.2, N 10.1, found: C 52.4, H 6.2, N 9.8.

Synthesis of 3-(4-(6-bromopyridin-2-yl)phenoxy)propan-1-ol (5). A solution of compound **2** (4.00 g, 16.1 mmol, 1.0 equiv.), K_2CO_3 (4.44 g, 32.1 mmol, 2.0 equiv.), KI (5.33 g, 32.1 mmol, 2.0 equiv.) and 3-chloro-1-propanol (3.04 g, 32.1 mmol, 2.0 equiv.) in acetonitrile (50 mL) was heated to reflux for 3 d. The solvent was removed and the residue was redissolved in water and ethyl acetate. The aqueous phase was extracted three times with ethyl acetate, the combined organic layers were dried ($MgSO_4$), and the solvent was removed *in vacuo*. The residue was purified by column chromatography (SiO_2, cyclohexane : ethyl acetate, 1 : 1). The product was obtained as a white solid. Yield: 58% (2.86 g, 9.28 mmol). ^{1}H NMR (400 MHz, DMSO-d_6): δ (ppm) = 8.04–7.96 (m, 2H, H-3), 7.93 (d, J = 7.8 Hz, 1H, H-10), 7.77 (t, J = 7.8 Hz, 1H, H-9), 7.50 (d, J = 7.8 Hz, 1H, H-8), 7.08–7.01 (m, 2H, H-2), 4.60–4.53 (m, 1H, H-14), 4.10 (t, J = 6.4 Hz, 2H, H-11), 3.62–3.53 (m, 2H, H-13), 1.94–1.83 (m, 2H, H-12). ^{13}C{^{1}H} NMR (101 MHz, DMSO-d_6): δ (ppm) = 160.1 (C-1), 157.2 (C-5), 141.1 (C-7), 140.3 (C-9), 129.0 (C-4), 128.0 (C-3), 125.5 (C-8), 118.5 (C-10), 114.6 (C-2), 64.7 (C-11), 57.1 (C-13), 32.0 (C-12). ^{15}N{^{1}H} NMR (41 MHz, DMSO-d_6): δ (ppm) = 305 (N-6). HRMS (m/z) $[C_{14}H_{14}BrNO_2 + Na]^+$: calcd: 330.0100, found: 330.0100. Elem. Anal. for $C_{14}H_{14}BrNO_2$ (%) calcd: C 54.6, H 4.6, N 4.6, found: C 54.6, H 4.7, N 4.4.

Synthesis of 3-(4-(6-ethynylpyridin-2-yl)phenoxy)propan-1-ol (6). A solution of compound **5** (2.00 g, 6.49 mmol, 1.0 equiv.) and trimethylsilyl acetylene (1.91 g, 19.5 mmol, 3.0 equiv.) in a mixture of triethyl amine (150 mL) and THF (50 mL) was purged with argon for 30 min. Subsequently, CuI (132 mg, 0.693 mmol, 0.1 equiv.) and $[PdCl_2(PPh_3)_2]$ (130 mg, 0.185 mmol, 0.3 equiv.) were added under an argon atmosphere, and the mixture was stirred overnight at 80 °C. It was then cooled to 0 °C, neutralized with aqueous HCl (4 M,

60 mL) and extracted three times with CH_2Cl_2. The combined organic layers were dried ($MgSO_4$). The solvent was removed *in vacuo* and the residue was filtered over Celite® and silica gel using diethyl ether. The solvent was removed *in vacuo*.

The crude product was then dissolved in a mixture of THF (20 mL) and CH_3OH (20 mL) and mixed with an aqueous solution of NaOH (20 mL, 1 M). The mixture was stirred for 1 h at room temperature and the solvent removed under reduced pressure. Water was added to the residue, and the product was extracted with CH_2Cl_2, the combined organic layers were dried ($MgSO_4$) and the filtrate was evaporated to dryness. The crude product was purified by column chromatography (SiO_2, cyclohexane : ethyl acetate, 1 : 1) and the product was obtained as a yellow solid. Yield: 80% (1.32 g, 5.21 mmol). ^{1}H NMR (400 MHz, DMSO-d_6): δ (ppm) = 8.08–8.00 (m, 2H, H-3), 7.94 (d, J = 8.1 Hz, 1H, H-10), 7.87 (t, J = 7.8 Hz, 1H, H-9), 7.47 (d, J = 7.5 Hz, 1H, H-8), 7.11–7.03 (m, 2H, H-2), 4.59 (t, J = 5.1 Hz, 1H, H-16), 4.35 (s, 1H, H-12), 4.13 (t, J = 6.4 Hz, 2H, H-13), 3.61 (q, J = 6.0 Hz, 2H, H-15), 1.92 (p, J = 6.3 Hz, 2H, H-14). ^{13}C{^{1}H} NMR (101 MHz, DMSO-d_6): δ (ppm) = 159.8 (C-1), 156.2 (C-5), 141.3 (C-7), 137.6 (C-9), 130.0 (C-4), 127.9 (C-3), 125.1 (C-8), 119.4 (C-10), 114.5 (C-2), 83.3 (C-11), 79.7 (C-12), 64.6 (C-13), 57.2 (C-15), 32.0 (C-15). ^{15}N{^{1}H} NMR (41 MHz, DMSO-d_6): δ (ppm) = 309 (N-6). HRMS (m/z) $[C_{16}H_{15}NO_2 + H]^+$: calcd: 254.1176, found: 254.1176. Elem. Anal. for $C_{16}H_{15}NO_2$ (%) calcd: C 75.9, H 6.0, N 5.5, found: C 75.4, H 6.1, N 5.1.

Synthesis of ^{OH}LH^{OH}. A solution of NaN_3 (2.16 g, 33.2 mmol, 2.0 equiv.) and 3-chloro-1-propanol (1.57 g, 16.6 mmol, 1.0 equiv.) in water (15 mL) was heated to reflux overnight. The product was extracted three times with CH_2Cl_2, the solvent was evaporated, and the crude product was used without further purification. The crude product, $CuSO_4{\cdot}5\ H_2O$ (1.66 g, 6.64 mmol, 0.2 equiv.), and sodium ascorbate (1.64 g, 8.30 mmol, 0.5 equiv.) were added to a solution of compound **6** (4.20 g, 16.6 mmol, 1.0 equiv.) in *tert*-butanol (15 mL), THF (15 mL) and water (15 mL). The solution was stirred for 1 d at room temperature. CH_2Cl_2 and a saturated aqueous solution of EDTA (30 mL) were then added. The aqueous phase was extracted three times with CH_2Cl_2. The combined organic layers were dried ($MgSO_4$), the solvent was removed under reduced pressure, and the crude product was purified by column chromatography (SiO_2, ethyl acetate : methanol, 100 : 2) to give the product as a beige solid. Yield: 75% (2.20 g, 6.21 mmol). ^{1}H NMR (500 MHz, DMSO-d_6): δ (ppm) = 8.74 (s, 1H, H-15), 8.18–8.12 (m, 2H, H-3), 7.95–7.87 (m, 2H, H-8, H-9), 7.86–7.81 (m, 1H, H-10), 7.08–7.02 (m, 2H, H-2), 4.70 (t, J = 5.0 Hz, 1H, H-19), 4.58 (t, J = 5.1 Hz, 1H, H-23), 4.52 (t, J = 7.1 Hz, 2H, H-16), 4.11 (t, J = 6.4 Hz, 2H, H-20), 3.63–3.56 (m, 2H, H-20), 3.49–3.42 (m, 2H, H-18), 2.06 (p, J = 6.5 Hz, 2H, H-17), 1.90 (p, J = 6.3 Hz, 2H, H-21). ^{13}C{^{1}H} NMR (126 MHz, DMSO-d_6): δ (ppm) = 159.7 (C-1), 155.4 (C-5), 149.6 (C-7), 147.3 (C-11), 138.0 (C-9), 130.5 (C-4), 127.9 (C-3), 123.4 (C-15), 118.1 (C-10), 117.0 (C-8), 114.4 (C-2), 64.6 (C-20), 57.4 (C-18), 57.2 (C-22), 46.8 (C-16), 32.8 (C-17), 32.0 (C-21). ^{15}N{^{1}H} NMR (51 MHz, DMSO-d_6): δ (ppm) = 364 (N-13), 348 (N-12), 297 (N-6), 253 (N-14). HRMS (m/z) $[C_{19}H_{22}N_4O_3 + H]^+$: calcd: 355.1765, found: 355.1765. Elem. Anal. for $C_{19}H_{22}N_4O_3$ (%) calcd: C 64.4, H 6.3, N 15.8, found: C 64.4, H 6.2, N 15.8.

Synthesis of ^{Cl}LH^{Cl}. A solution of ^{OH}LH^{OH} (450 mg, 1.27 mmol, 1.0 equiv.) in dry CH_2Cl_2 (8 mL) was cooled to 0 °C. Thionyl chloride (737 μL, 10.2 mmol, 8.0 equiv.) was added dropwise. The mixture was stirred at 50 °C for 18 h. After carefully adding water (20 mL), the crude product was extracted with CH_2Cl_2. The organic layer was dried ($MgSO_4$) and evaporated to dryness. The crude product was purified by column chromatography (SiO_2, cyclohexane : ethyl acetate, 8 : 2). The product was obtained as white solid. Yield: 95% (474 mg, 1.21 mmol). ^{1}H NMR (500 MHz, $CDCl_3$): δ (ppm) = 8.29 (s, 1H, H-15), 8.06 (d, J = 7.9 Hz, 1H, H-8), 8.04–7.99 (m, 2H, H-3), 7.81 (t, J = 7.9 Hz, 1H, H-9), 7.62 (d, J = 7.9 Hz, 1H, H-10), 7.04–6.98 (m, 2H, H-2), 4.63 (t, J = 6.6 Hz, 2H, H-16), 4.19 (t, J = 5.8 Hz, 2H, H-19), 3.77 (t, J = 6.3 Hz, 2H, H-21), 3.58 (t, J = 6.1 Hz, 2H, H-18), 2.46 (p, J = 6.4 Hz, 2H, H-17), 2.27 (p, J = 6.1 Hz, 2H, H-20). ^{13}C{^{1}H} NMR (126 MHz, $CDCl_3$): δ (ppm) = 159.7 (C-1), 156.5 (C-5), 149.8 (C-7), 148.9 (C-11), 137.6 (C-9), 132.0 (C-4), 128.2 (C-3), 122.7 (C-15), 118.8 (C-10), 117.8 (C-8), 114.7 (C-2), 64.4 (C-19), 47.2 (C-16), 41.5 (C-21), 41.1 (C-18), 32.6 (C-17), 32.2 (C-20). ^{15}N{^{1}H} NMR (51 MHz, $CDCl_3$): δ (ppm) = 363 (N-13), 348 (N-12), 246 (N-14). HRMS (m/z) $[C_{19}H_{20}Cl_2N_4O + H]^+$: calcd: 391.1087, found: 391.1079. Elem. Anal. for $C_{19}H_{20}Cl_2N_4O$ (%) calcd: C 58.3, H 5.2, N 14.3, found: C 58.4 H 5.4, N 14.1.

Synthesis of 2-(4-(3-bromopropoxy)phenyl)-6-(1-(3-bromopropyl)-1*H*-1,2,3-triazol-4-yl)pyridine 7. A solution of ^{OH}LH^{OH} (471 mg, 1.33 mmol, 1.0 equiv.) and PPh_3 (1.04 g, 3.98 mmol, 3.0 equiv.) in dry CH_2Cl_2 (30 mL) was cooled to 0 °C and *N*-bromosuccinimide (709 mg, 3.98 mmol, 3.0 equiv.) was added in portions. The mixture was stirred overnight at room temperature. After careful addition of water (20 mL), the crude product was extracted with CH_2Cl_2. The organic layer was dried ($MgSO_4$) and the filtrate was evaporated to dryness. The crude product was purified by column chromatography (SiO_2, cyclohexane : ethyl acetate, 7 : 3). The product was obtained as white solid. Yield: 61% (392 mg, 0.816 mmol). ^{1}H NMR (400 MHz, $CDCl_3$): δ (ppm) = 8.32 (s, 1H, H-15), 8.07 (d, J = 7.8 Hz, 1H, H-8), 8.04–7.98 (m, 2H, H-3), 7.81 (d, J = 7.8 Hz, 1H, H-9), 7.61 (d, J = 7.9 Hz, 1H, H-10), 7.05–6.98 (m, 2H, H-2), 4.62 (t, J = 6.6 Hz, 2H, H-16), 4.17 (t, J = 5.8 Hz, 2H, H-19), 3.62 (t, J = 6.4 Hz, 2H, H-21), 3.41 (d, J = 6.2 Hz, 2H, H-18), 2.53 (p, J = 6.4 Hz, 2H, H-17), 2.35 (p, J = 6.1 Hz, 2H, H-20). ^{13}C{^{1}H} NMR (101 MHz, $CDCl_3$): δ (ppm) = 159.7 (C-1), 156.6 (C-5), 149.8 (C-7), 148.8 (C-11), 137.7 (C-9), 131.9 (C-4), 128.3 (C-3), 122.8 (C-15), 118.9 (C-10), 117.9 (C-8), 114.7 (C-2), 65.5 (C-19), 48.4 (C-16), 32.7 (C-17), 32.4 (C-20), 30.0 (C-21), 29.4 (C-18). ^{15}N{^{1}H} NMR (41 MHz, $CDCl_3$): δ (ppm) = 363 (N-13), 348 (N-12), 294 (N-6), 247 (N-14). HRMS (m/z) $[C_{19}H_{20}Br_2N_4O + H]^+$: calcd: 479.0077, found: 479.0077. Elem. Anal. for $C_{19}H_{20}Br_2N_4O$ (%) calcd: C 47.5, H 4.2, N 11.7, found: C 47.6, H 4.3, N 11.7.

Synthesis of ^{M}LH^{M}. A suspension of compound 7 (830 mg, 1.73 mmol, 1.0 equiv.), K_2CO_3 (954 mg, 6.91 mmol, 4.0 equiv.), and morpholine (602 mg, 6.91 mmol, 4.0 equiv.) in acetonitrile

(20 mL) was heated to reflux overnight. Subsequently, the solvent was removed under reduced pressure. The crude product was purified by column chromatography (SiO_2, CH_2Cl_2 : CH_3OH, 100 : 5), yielding this product as a beige solid. Yield: 82% (704 mg, 1.42 mmol). ^{1}H NMR (400 MHz, CD_2Cl_2): δ (ppm) = 8.29 (s, 1H, H-15), 8.06–8.02 (m, 2H, H-3), 8.01 (dd, J = 7.8, 1.0 Hz, 1H, H-8), 7.81 (t, J = 7.8 Hz, 1H, H-9), 7.63 (dd, J = 8.0, 1.0 Hz, 1H, H-10), 7.05–6.98 (m, 2H, H-2), 4.51 (t, J = 7.0 Hz, 2H, H-16), 4.10 (t, J = 6.4 Hz, 2H, H-22), 3.72–3.64 (m, 8H, H-27, H-21), 2.52 (t, J = 7.1 Hz, 2H, H-24), 2.47–2.39 (m, 8H, H-26, H-20), 2.36 (t, J = 6.7 Hz, 2H, H-18), 2.18–2.07 (m, 2H, H-17), 2.03–1.92 (m, 2H, H-23). ^{13}C{^{1}H} NMR (101 MHz, CD_2Cl_2): δ (ppm) = 160.5 (C-1), 156.8 (C-5), 150.6 (C-7), 148.9 (C-11), 137.9 (C-9), 132.0 (C-4), 128.4 (C-3), 123.0 (C-15), 118.8 (C-10), 117.8 (C-8), 114.9 (C-2), 67.4 (C-27), 67.3 (C-21), 66.7 (C-22), 55.7 (C-24), 55.4 (C-18), 54.2 (C-26), 54.0 (C-20), 48.6 (C-16), 27.4 (C-17), 26.9 (C-23). ^{15}N{^{1}H} NMR (41 MHz, CD_2Cl_2): δ (ppm) = 364 (N-13), 347 (N-12), 295 (N-6), 250 (N-14). HRMS (m/z) $[C_{27}H_{36}N_6O_3 + H]^+$: calcd: 493.2922, found: 493.2922. Elem. Anal. for $C_{27}H_{36}N_6O_3$ (%) calcd: C 65.8, H 7.4, N 17.1, found: C 65.9, H 7.3, N 17.1.

Synthesis of [PtCl(^{P}L)]. A solution of ^{P}LH (500 mg, 1.30 mmol, 1.0 equiv.) in 2-ethoxyethanol (15 mL) and water (15 mL) was purged with argon for 30 min, then K_2PtCl_4 (537 mg, 1.30 mmol, 1.0 equiv.) was added, and the mixture was stirred at 80 °C for 1 d under an argon atmosphere. The resulting precipitate was filtered, washed with water, ethanol, and diethyl ether, and dried under vacuum. The complex was obtained as a yellow solid. Yield: 75% (602 mg, 0.977 mmol). ^{1}H NMR (500 MHz, DMF-d_7): δ (ppm) = 9.22 (s, 1H, H-17), 8.08 (t, J = 8.0 Hz, 1H, H-11), 7.86 (d, J = 7.8 Hz, 1H, H-12), 7.82 (d, J = 7.7 Hz, 1H, H-10), 7.71 (d, J = 7.5 Hz, 1H, H-2), 7.60 (d, J = 7.6 Hz, 1H, H-5), 7.17 (t, J = 7.5 Hz, 1H, H-3), 7.09 (t, J = 7.4 Hz, 1H, H-4), 4.86 (dt, J = 12.8, 7.7 Hz, 2H, H-18), 4.19–4.05 (m, 4H, H-21), 2.73–2.64 (m, 2H, H-19), 1.28 (t, J = 7.0 Hz, 6H, H-22). ^{13}C{^{1}H} NMR (126 MHz, DMF-d_7): δ (ppm) = 166.4 (d, $^2J_{C,Pt}$ = 108 Hz, C-7), 150.0 (d, $^2J_{C,Pt}$ = 61 Hz, C-13), 148.9 (d, $^2J_{C,Pt}$ = 12 Hz, C-9), 147.5 (d, $^2J_{C,Pt}$ = 69 Hz, C-6), 140.7 (C-1, C-11), 134.5 (d, $^2J_{C,Pt}$ = 52 Hz, C-2), 130.6 (C-3), 127.1 (C-17), 125.4 (d, $^3J_{C,Pt}$ = 43 Hz, C-5), 124.6 (C-4), 118.4 (d, $^3J_{C,Pt}$ = 44 Hz, C-12), 118.1 (d, $^3J_{C,Pt}$ = 25 Hz, C-10), 62.4 (d, $^2J_{C,P}$ = 6.2 Hz, C-21), 47.4 (d, $^2J_{C,P}$ = 1.7 Hz, C-18), 26.4 (d, $^1J_{C,P}$ = 13.2 Hz, C-19), 16.6 (d, $^3J_{C,P}$ = 5.9 Hz, C-22). ^{15}N{^{1}H} NMR (51 MHz, DMF-d_7): δ (ppm) = 360 (N-15), 302 (N-14), 250 (N-16), 222 (N-8). ^{31}P{^{1}H} NMR (202 MHz, DMF-d_7): δ (ppm) = 25.5 (P-20). ^{195}Pt{^{1}H} NMR (107 MHz, DMF-d_7): δ (ppm) = −3498. HRMS (m/z) $[C_{19}H_{22}ClN_4O_3PPt + Na]^+$: calcd: 638.0658, found: 638.0661. Elem. Anal. for $C_{19}H_{22}ClN_4O_3PPt$ (%) calcd: C 37.1, H 3.6, N 9.1, found: C 37.1, H 3.7, N 9.1.

Synthesis of [Pt(A)(^{P}L)]. The general procedure for the synthesis of complexes with auxiliary ligand A was applied to [PtCl(^{P}L)] (200 mg, 0.325 mmol), and the crude product was purified by column chromatography (SiO_2, CH_2Cl_2 : CH_3OH, 100 : 3). The product was obtained as a yellow solid. Yield: 56% (123 mg, 0.180 mmol). ^{1}H NMR (500 MHz, CD_2Cl_2): δ (ppm) = 8.25 (s, 1H, H-17), 7.93 (d, $^3J_{H,Pt}$ = 99 Hz, J = 7.5 Hz, 1H, H-2), 7.53–7.45 (m, 2H, H-26), 7.41 (t, J = 7.9 Hz, 1H, H-11), 7.33–7.29 (m, 2H, H-27), 7.29–7.26 (m, 1H, H-5), 7.23 (d, J = 8.2 Hz, 1H, H-12), 7.21–7.17 (m, 1H, H-28), 7.15 (t, J = 7.4 Hz, 1H, H-3), 7.09 (d, J = 7.7 Hz, 1H, H-10), 7.05 (t, J = 7.5 Hz, 1H, H-4), 4.70 (dt, $^3J_{H,P}$ = 13.5, J = 7.6 Hz, 2H, H-18), 4.02 (dq, $^3J_{H,P}$ = 8.3, J = 7.1 Hz, 4H, H-21), 2.47 (dt, $^2J_{H,P}$ = 18.4, J = 7.6 Hz, 2H, H-19), 1.25 (t, J = 7.1 Hz, 6H, H-22). ^{13}C{^{1}H} NMR (126 MHz, CD_2Cl_2): δ (ppm) = 163.4 ($^2J_{C,Pt}$ = 99 Hz, C-7), 150.5 ($^2J_{C,Pt}$ = 50 Hz, C-13), 146.7 (C-9), 146.0 ($^2J_{C,Pt}$ = 36 Hz, C-6), 139.2 ($^1J_{C,Pt}$ = 1124 Hz, C-1), 138.5 (C-11), 136.8 ($^2J_{C,Pt}$ = 99 Hz, C-2), 130.9 (C-26), 130.2 ($^3J_{C,Pt}$ = 75 Hz, C-3), 128.3 (C-25), 127.5 (C-27), 124.9 (C-17), 124.5 (C-28), 123.8 ($^3J_{C,Pt}$ = 43 Hz, C-5), 123.1 (C-4), 116.3 (C-10), 116.2 (C-12), 104.3 ($^2J_{C,Pt}$ = 410 Hz, C-24), 101.8 ($^1J_{C,Pt}$ = 1541 Hz, C-23), 61.6 (d, $^2J_{C,P}$ = 6.5 Hz, C-21), 46.2 (d, $^2J_{C,P}$ = 1.7 Hz, C-18), 25.8 (d, $^1J_{C,P}$ = 141.2 Hz, C-19), 15.6 (d, $^3J_{C,P}$ = 5.8 Hz, C-22). ^{15}N{^{1}H} NMR (51 MHz, CD_2Cl_2): δ (ppm) = 359 (N-15), 298 (N-14), 248 (N-16), 245 (N-8). ^{31}P{^{1}H} NMR (202 MHz, CD_2Cl_2): δ (ppm) = 24.7 (P-20). ^{195}Pt{^{1}H} NMR (107 MHz, CD_2Cl_2): δ (ppm) = −3870. HRMS (m/z) $[C_{27}H_{27}N_4O_3PPt + H]^+$: calcd: 682.1544, found: 682.1550. Elem. Anal. for $C_{27}H_{27}N_4O_3PPt$ (%) calcd: C 47.6, H 4.0, N 8.2, found: C 48.1, H 4.4, N 7.7.

Synthesis of [Pt(B)(^{P}L)]OTf. The general procedure for the synthesis of complexes with auxiliary ligand B was applied to [PtCl(^{P}L)] (150 mg, 0.244 mmol), with the complex isolated as an orange solid. Yield: 51% (103 mg, 0.125 mmol). ^{1}H NMR (400 MHz, DMSO-d_6): δ (ppm) = 9.15 (s, 1H, H-17), 8.12 (t, J = 8.0 Hz, 1H, H-11), 7.93 (dd, J = 8.2, J = 0.9 Hz, 1H, H-12), 7.85 (dd, J = 7.7 Hz, J = 0.9 Hz, 1H, H-10), 7.68–7.58 (m, 2H, H-2, H-5), 7.13–7.01 (m, 2H, H-2, H-3), 4.72 (td, J = 7.4 Hz, $^3J_{H,P}$ = 7.1 Hz, 2H, H-18), 4.39 (s, 2H, H-25), 4.08–3.95 (m, 4H, H-21), 3.15 (s, 9H, H-27), 2.58 (dt, $^2J_{H,P}$ = 18.1 Hz, J = 7.4 Hz, 2H, H-19), 1.21 (t, J = 7.0 Hz, 6H, H-22). ^{13}C{^{1}H} NMR (101 MHz, DMSO-d_6): δ (ppm) = 163.9 (C-7), 150.4 (C-13), 147.5 (C-9), 146.7 (C-6), 141.2 (C-11), 139.5 (C-1), 137.0 (C-2), 130.6 (C-3), 126.5 (C-17), 125.2 (C-5), 123.8 (C-4), 117.9 (C-12), 117.3 (C-10), 104.3 (C-23), 89.7 (C-24), 61.4 (d, $^2J_{C,P}$ = 6.2 Hz, C-21), 59.1 (C-25), 50.9 (t, $^1J_{C,N}$ = 4.1 Hz, C-27), 46.3 (C-18), 25.1 (d, $^1J_{C,P}$ = 139.4 Hz, C-19), 16.1 (d, $^3J_{C,P}$ = 5.8 Hz, C-22). ^{15}N{^{1}H} NMR (41 MHz, DMSO-d_6): δ (ppm) = 296 (N-14), 251 (N-16), 243 (N-8), 53 (N 26). ^{19}F{^{1}H} NMR (376 MHz, DMSO-d_6): δ (ppm) = −77.7. ^{31}P{^{1}H} NMR (162 MHz, DMSO-d_6): δ (ppm) = 25.9 (P-20). ^{195}Pt{^{1}H} NMR (86 MHz, DMSO-d_6): δ (ppm) = −3914. HRMS (m/z) $[C_{25}H_{33}N_5O_3PPt]^+$: calcd: 677.1963, found: 677.1992.

Synthesis of [PtCl(^{M}L)]. ^{M}LH (424 mg, 1.21 mmol, 1.0 equiv.) was dissolved in acetic acid (50 mL) and the solution was purged with argon for 30 min. K_2PtCl_4 (503 mg, 1.21 mmol, 1.0 equiv.) was added, and the mixture was stirred at 120 °C for 3 d under an argon atmosphere. The precipitate was filtered, washed with water, ethanol, and diethyl ether, and dried under vacuum. The complex was obtained as a yellow solid. Yield: 46% (324 mg, 0.560 mmol). ^{1}H NMR (400 MHz, DMF-d_7): δ (ppm) = 9.71 (s, 1H, H-17), 8.09 (t, J = 7.9 Hz, 1H, H-11), 7.92 (d, J = 7.3 Hz, 1H, H-10), 7.85 (d, J = 8.1 Hz, 1H, H-12), 7.70 (d, J = 7.6 Hz, 1H, H-2), 7.61 (d, J = 7.7 Hz, 1H, H-5), 7.17

(t, J = 7.5 Hz, 1H, H-3), 7.09 (t, J = 7.4 Hz, 1H, H-4), 4.98 (t, J = 7.0 Hz, 2H, H-18), 4.17–3.96 (m, 4H, H-23), 3.87–3.77 (m, 2H, H-22), 3.76–3.63 (m, 2H, H-20), 3.45–3.25 (m, 2H, H-22), 3.02–2.93 (m, 2H, H-19). $^{13}C\{^1H\}$ NMR (101 MHz, DMF-d_7): δ (ppm) = 166.3 (C-7), 150.1 (C-13), 149.0 (C-9), 147.5 (C-6), 140.7 (C-11), 140.6 (C-1), 134.5 (C-2), 130.5 (C-3), 127.4 (C-17), 125.4 (C-5), 124.6 (C-4), 118.4 (C-10), 118.3 (C-12), 64.5 (C-23), 54.5 (C-20), 52.8 (C-22), 49.9 (C-18), 24.9 (C-19). $^{195}Pt\{^1H\}$ NMR (86 MHz, DMF-d_7): δ (ppm) = −3500. HRMS (m/z) $[C_{20}H_{22}N_5OPtCl + H]^+$: calcd: 579.1233, found: 579.1235. Elem. Anal. for $C_{20}H_{22}N_5OPtCl{\cdot}0.5\ CH_3COOH{\cdot}3.5\ HCl$ (%) calcd: C 34.2, H 3.8, N 9.5, found: C 34.1, H 3.7, N 9.3.

Synthesis of [Pt(A)(^{M}L)]. The general procedure for the synthesis of complexes with auxiliary ligand B was applied to [PtCl(^{M}L)] (70 mg, 0.12 mmol, 1.0 equiv.), with purification by column chromatography (SiO_2, CH_2Cl_2 : CH_3OH, 100 : 4). The product was obtained as a red solid. Yield: 41% (32 mg, 50 μmol). ^1H NMR (400 MHz, CD_2Cl_2): δ (ppm) = 8.22 (s, 1H, H-17), 7.97 (d, J = 7.3 Hz, 1H, H-2), 7.51–7.45 (m, 2H, H-27), 7.42 (t, J = 7.9 Hz, 1H, H-11), 7.34–7.22 (m, 3H, H-5, H-28), 7.22–7.13 (m, 3H, H-3, H-12, H-29), 7.12–7.03 (m, 2H, H-4, H-10), 4.54 (t, J = 7.2 Hz, 2H, H-18), 3.59 (t, J = 4.6 Hz, 4H, H-23), 2.34–2.24 (m, 6H, H-20, H-22), 2.10 (p, J = 6.8 Hz, 2H, H-19). $^{13}C\{^1H\}$ NMR (101 MHz, CD_2Cl_2): δ (ppm) = 164.6 ($^2J_{C,Pt}$ = 99 Hz, C-7), 151.3 ($^2J_{C,Pt}$ = 40 Hz, C-13), 147.9 (C-9), 147.0 ($^2J_{C,Pt}$ = 38 Hz, C-6), 140.3 ($^1J_{C,Pt}$ = 1124 Hz, C-1), 139.4 (C-11), 137.9 ($^2J_{C,Pt}$ = 100 Hz, C-2), 131.8 (C-27), 131.3 ($^3J_{C,Pt}$ = 73 Hz, C-3), 129.4 (C-26), 128.5 (C-28), 125.6 (C-17), 125.5 (C-29), 124.8 ($^3J_{C,Pt}$ = 45 Hz, C-5), 124.1 (C-4), 117.2 (C-12), 117.1 (C-10), 105.4 ($^2J_{C,Pt}$ = 408 Hz, C-25), 102.8 ($^1J_{C,Pt}$ = 1540 Hz, C-24), 67.2 (C-23), 55.3 (C-20), 53.9 (C-22), 50.9 (C-18), 30.08, 26.7 (C-19). $^{15}N\{^1H\}$ NMR (41 MHz, CD_2Cl_2): δ (ppm) = 359 (N-15), 297 (N-14), 250 (N-16), 245 (N-8). $^{195}Pt\{^1H\}$ NMR (86 MHz, CD_2Cl_2): δ (ppm) = −3869. HRMS (m/z) $[C_{28}H_{27}N_5OPt + H]^+$: calcd: 645.1938, found: 645.1931. Elem. Anal. for $C_{28}H_{27}N_5OPt$ (%) calcd: C 52.2, H 4.2, N 10.9, found: C 51.9, H 4.4, N 10.6. Single crystals for X-ray structure analysis were obtained by slow diffusion of diethyl ether into a concentrated solution of the complex in DMF.

Synthesis of [Pt(B)(^{M}L)]OTf. The general procedure for the synthesis of complexes with auxiliary ligand B was applied to [PtCl(^{M}L)] (150 mg, 0.259 mmol). The complex was isolated as an orange solid. Yield: 38% (77 mg, 0.10 mmol). ^1H NMR (400 MHz, DMSO-d_6): δ (ppm) = 9.11 (s, 1H, H-17), 8.12 (t, J = 8.0 Hz, 1H, H-11), 7.92 (d, J = 8.6 Hz, 1H, H-12), 7.84 (d, J = 7.8 Hz, 1H, H-10), 7.67–7.62 (m, 2H, H-2, H-5), 7.16–7.06 (m, 2H, H-3, H-4), 4.61 (s, 2H, H-18), 4.39 (s, 2H, H-26), 3.59 (s, 4H, H-23), 3.16 (s, 9H, H-28), 2.33 (t, J = 1.9 Hz, 4H, H-22), 2.16 (s, 2H, H-19). $^{13}C\{^1H\}$ NMR (101 MHz, DMSO-d_6): δ (ppm) = 163.8 (C-7), 150.5 (C-13), 147.6 (C-9), 146.7 (C-6), 141.1 (C-11), 139.5 (C-1), 137.0 (C-2), 130.5 (C-3), 126.4 (C-17), 125.1 (C-5), 123.8 (C-4), 117.8 (C-12), 117.3 (C-10), 104.4 (C-24), 89.7 (C-25), 66.0 (C-23), 59.1 (C-26), 54.5 (C-20), 52.9 (C-22), 51.0 (C-28), 50.9 (C-18), 24.4 (C-19). $^{15}N\{^1H\}$ NMR (41 MHz, DMSO-d_6): δ (ppm) = 296 (N-14), 253 (N-16), 243 (N-8), 53 (N 27). $^{19}F\{^1H\}$ NMR (376 MHz, DMSO-d_6): δ (ppm) = −77.7. $^{195}Pt\{^1H\}$ NMR (86 MHz, DMSO-d_6): δ (ppm) = −3913. HRMS (m/z) $[C_{26}H_{33}N_6OPt]^+$: calcd: 640.2358, found: 640.2369.

Synthesis of [Pt(A)(^{OH}L)]. The general procedure for the synthesis of complexes with auxiliary ligand B was applied to [PtCl(^{OH}L)][73] (100 mg, 0.196 mmol, 1.0 equiv.), with purification by column chromatography (Al_2O_3, CH_2Cl_2 : CH_3OH, 100 : 2). The product was obtained as a yellow solid. Yield: 33% (38 mg, 0.66 μmol). ^1H NMR (400 MHz, DMSO-d_6): δ (ppm) = 9.13 (s, 1H, H-17), 8.08 (t, J = 8.0 Hz, 1H, H-11), 7.90 (d, J = 8.3 Hz, 1H, H-12), 7.87–7.80 (m, 2H, H-10, H-2), 7.62 (dd, J = 7.5, J = 1.6 Hz, 1H, H-5), 7.33–7.24 (m, 4H, H-26, H-25), 7.17–7.03 (m, 3H, H-27, H-4, H-3), 4.77 (t, J = 4.9 Hz, 1H, H-21), 4.62 (t, J = 7.1 Hz, 2H, H-18), 3.52–3.45 (m, 2H, H-20), 2.15–2.04 (m, 2H, H-19). $^{13}C\{^1H\}$ NMR (101 MHz, DMSO-d_6): δ (ppm) = 163.7 (C-7), 150.6 (C-13), 147.5 (C-9), 146.6 (C-6), 140.6 (C-11), 139.7 (C-1), 137.0 ($^2J_{C,Pt}$ = 93 Hz, C-2), 130.8 (C-25), 130.3 (C-3), 128.9 (C-24), 128.0 (C-26), 126.2 (C-17), 124.9 (C-5), 124.6 (C-27), 123.5 (C-4), 117.5 (C-12), 117.2 (C-10), 104.5 (C-22), 104.3 (C-23), 57.2 (C-20), 48.9 (C-18), 32.1 (C-19). $^{15}N\{^1H\}$ NMR (41 MHz, DMSO-d_6): δ (ppm) = 361 (N-15), 296 (N-14), 252 (N-16), 245 (N-8). $^{195}Pt\{^1H\}$ NMR (86 MHz, DMSO-d_6): δ (ppm) = −3894. HRMS (m/z) $[C_{24}H_{20}N_4OPt + H]^+$: calcd: 576.1360, found: 576.1368. Elem. Anal. for $C_{24}H_{20}N_4OPt{\cdot}0.125\ AgCl$ (%) calcd: C 48.6, H 3.4, N 9.4, found: C 48.8, H 3.7, N 9.4.

Synthesis of [Pt(B)(^{OH}L)]OTf. The general procedure for the synthesis of complexes with auxiliary ligand B was applied to [PtCl(^{OH}L)][73] (150 mg, 0.294 mmol). The complex was isolated as a beige solid. Yield: 22% (46 mg, 64 μmol). ^1H NMR (400 MHz, DMSO-d_6): δ (ppm) = 9.13 (s, 1H, H-17), 8.08 (t, J = 8.0 Hz, 1H, H-11), 7.89 (d, J = 8.1 Hz, 1H, H-12), 7.82 (d, J = 7.8 Hz, 1H, H-10), 7.68–7.60 (m, 2H, H-2, H-5), 7.16–7.03 (m, 2H, H-3, H-4), 4.81 (t, J = 5.0 Hz, 1H, H-21), 4.59 (t, J = 7.0 Hz, 2H, H-18), 4.41 (s, 2H, H-24), 3.56–3.46 (m, 2H, H-20), 3.16 (s, 9H, H-26), 2.17–2.01 (m, 2H, H-19). $^{13}C\{^1H\}$ NMR (101 MHz, DMSO-d_6): δ (ppm) = 163.7 (d, $^2J_{C,Pt}$ = 98 Hz, C-7), 150.5 (d, $^2J_{C,Pt}$ = 38 Hz, C-13), 147.6 (C-9), 146.7 (C-6), 141.0 (C-11), 139.6 (d, $^1J_{C,Pt}$ = 1117 Hz, C-1), 136.9 (d, $^2J_{C,Pt}$ = 98 Hz, C-2), 130.5 (C-3), 126.3 (C-17), 125.1 (d, $^3J_{C,Pt}$ = 40 Hz, C-5), 123.7 (C-4), 120.6 (q, $^1J_{C,F}$ = 322 Hz, CF_3), 117.7 (C-12), 117.3 (C-10), 104.4 (d, $^1J_{C,Pt}$ = 1538 Hz, C-22), 89.7 (d, $^2J_{C,Pt}$ = 41.5 Hz, C-23), 59.0 (t, $^1J_{C,^{14}N}$ = 2.7 Hz, $^3J_{C,Pt}$ = 25 Hz, C-24), 57.1 (C-20), 50.9 (t, $^1J_{C,^{14}N}$ = 3.7 Hz, C-26), 48.9 (C-18), 32.0 (C-19). $^{15}N\{^1H\}$ NMR (41 MHz, DMSO-d_6): δ (ppm) = 361 (N-15), 297 (N-14), 253 (N-16), 244 (N-8), 53 (N 25). $^{19}F\{^1H\}$ NMR (376 MHz, DMSO-d_6): δ (ppm) = −77.7. $^{195}Pt\{^1H\}$ NMR (86 MHz, DMSO-d_6): δ (ppm) = −3911. HRMS (m/z) $[C_{22}H_{26}N_5OPt]^+$: calcd: 571.1780, found: 571.1801.

Synthesis of [PtCl(^{Cl}L)]. A solution of ^{Cl}LH (530 mg, 1.77 mmol, 1.0 equiv.) in acetic acid (40 mL) was purged with argon for 30 min, then K_2PtCl_4 (738 mg, 1.78 mmol, 1.0 equiv.) was added, and the mixture was stirred at 120 °C under an argon atmosphere for 3 d. The resulting precipitate was filtered, washed with water, ethanol, and diethyl ether, and dried under vacuum. The complex was obtained as a yellow solid. Yield: 83% (784 mg, 1.48 mmol). ^1H NMR (400 MHz, DMF-d_7):

δ (ppm) = 9.18 (s, 1H, H-17), 8.04 (t, J = 8.0 Hz, 1H, H-11), 7.83 (d, J = 8.3 Hz, 1H, H-12), 7.78 (d, J = 7.8 Hz, 1H, H-10), 7.70 (d, J = 7.5 Hz, 1H, H-2), 7.59 (d, J = 7.8 Hz, 1H, H-5), 7.16 (d, J = 7.6 Hz, 1H, H-3), 7.08 (d, J = 7.5 Hz, 1H, H-4), 4.80 (t, J = 6.9 Hz, 2H, H-18), 3.84 (t, J = 6.4 Hz, 2H, H-20), 2.54 (p, J = 6.7 Hz, 2H, H-19). $^{13}C\{^1H\}$ NMR (101 MHz, DMF-d_7): δ (ppm) = 166.4 ($^2J_{C,Pt}$ = 109 Hz, C-7), 150.4 ($^2J_{C,Pt}$ = 64 Hz, C-13), 149.1 ($^2J_{C,Pt}$ = 13 Hz, C-9), 147.7 ($^2J_{C,Pt}$ = 70 Hz, C-6), 140.9 ($^1J_{C,Pt}$ = 1116 Hz, C-1), 140.8 (C-11), 134.7 ($^2J_{C,Pt}$ = 53 Hz, C-10), 130.7 ($^3J_{C,Pt}$ = 53 Hz, C-3), 127.3 (C-17), 125.5 ($^3J_{C,Pt}$ = 43 Hz, C-5), 124.7 (C-4), 118.5 ($^3J_{C,Pt}$ = 46 Hz, C-12), 118.4 ($^3J_{C,Pt}$ = 24 Hz, C-10), 50.3 (C-18), 42.6 (C-20), 33.1 (C-19). $^{15}N\{^1H\}$ NMR (41 MHz, DMF-d_7): δ (ppm) = 360 (N-15), 302 (N-13), 250 (N-16), 222 (N-8). $^{195}Pt\{^1H\}$ NMR (86 MHz, DMF-d_7): δ (ppm) = −3498. HRMS (m/z) $[C_{16}H_{14}N_4Cl_2Pt + Na]^+$: calcd: 550.0135, found: 550.0141. Elem. Anal. for $C_{16}H_{14}N_4Cl_2Pt$ (%) calcd: C 36.4, H 2.7, N 10.6, found: C 36.6, H 2.8, N 10.6.

Synthesis of [Pt(A)(^{Cl}L)]. The general procedure for the synthesis of complexes with auxiliary ligand A was applied to [PtCl(^{Cl}L)] (300 mg, 0.568 mmol), and the crude product was purified by column chromatography (Al_2O_3, CH_2Cl_2 : CH_3OH, 100 : 0.3). The product was obtained as a yellow solid. Yield: 61% (119 mg, 0.200 mmol). ^1H NMR (400 MHz, CD_2Cl_2): δ (ppm) = 8.20 (s, 1H, H-17), 8.03–7.80 (m, 1H, H-2), 7.49–7.44 (m, 2H, H-24), 7.38–7.33 (m, 1H, H-11), 7.33–7.26 (m, 3H, H-5, H-25), 7.23–7.12 (m, 3H, H-3, H-12, H-26), 7.10–7.03 (m, 2H, H-4, H-10), 4.66 (t, J = 7.0 Hz, 2H, H-18), 3.53 (t, J = 6.1 Hz, 2H, H-20), 2.49–2.38 (m, 2H, H-19). $^{13}C\{^1H\}$ NMR (101 MHz, CD_2Cl_2): δ (ppm) = 164.4 (C-7), 151.6 (C-13), 147.7 (C-9), 147.0 (C-6), 140.1 (C-1), 139.3 (C-11), 137.9 (C-2), 131.8 (C-24), 131.3 (C-3), 129.2 (C-23), 128.6 (C-25), 125.8 (C-17), 125.6 (C-26), 124.8 (C-5), 124.1 (C-4), 117.4 (C-10), 117.1 (C-12), 105.4 (C-22), 102.6 (C-21), 49.9 (C-18), 41.7 (C-20), 32.3 (C-19). $^{15}N\{^1H\}$ NMR (41 MHz, CD_2Cl_2): δ (ppm) = 359 (N-15), 298 (N-14), 247 (N-16), 245 (N-8). $^{195}Pt\{^1H\}$ NMR (86 MHz, CD_2Cl_2): δ (ppm) = −3866. HRMS (m/z) $[C_{24}H_{19}N_4ClPt + H]^+$: calcd: 594.1021, found: 594.1014. Elem. Anal. for $C_{24}H_{19}N_4ClPt$ (%) calcd: C 48.5, H 3.2, N 9.4, found: C 48.9, H 3.3, N 9.3. Single crystals for X-ray structure analysis were obtained by slow diffusion of diethyl ether into a concentrated solution of the complex in DMF.

Synthesis of [Pt(B)(^{Cl}L)]OTf. The general procedure for the synthesis of complexes with auxiliary ligand B was applied to [PtCl(^{Cl}L)] (200 mg, 0.379 mmol). The complex was isolated as an orange solid. Yield: 44% (124 mg, 0.168 mmol). ^1H NMR (500 MHz, DMSO-d_6): δ (ppm) = 9.10 (s, 1H, H-17), 8.10 (t, J = 7.9 Hz, 1H, H-11), 7.90 (d, J = 8.1 Hz, 1H, H-12), 7.81 (d, J = 7.8 Hz, 1H, H-10), 7.73–7.52 (m, 2H, H-2, H-5), 7.15–7.03 (m, 2H, H-3, H-4), 4.66 (t, J = 6.8 Hz, 2H, H-18), 4.39 (s, 2H, H-23), 3.74 (t, J = 6.3 Hz, 2H, H-20), 3.15 (s, 9H, H-25), 2.45–2.36 (m, 2H, H-19). $^{13}C\{^1H\}$ NMR (126 MHz, DMSO-d_6): δ (ppm) = 163.7 (C-7), 150.5 ($^2J_{C,Pt}$ = 38 Hz, C-13), 147.4 (C-9), 146.6 (C-6), 140.9 (C-11), 139.5 (C-1), 136.9 (C-2), 130.5 (C-3), 126.3 (C-17), 125.0 (C-5), 123.7 (C-4), 120.5 (q, $^1J_{C,F}$ = 322 Hz, CF_3), 117.7 (C-12), 117.3 (C-10), 104.4 (C-21), 89.6 (C-22), 59.1 (C-23), 50.8 (t, $^1J_{C,N}$ = 4.0 Hz, C-25), 48.9 (C-18), 41.7 (C-20), 31.5 (C-19). $^{15}N\{^1H\}$ NMR (51 MHz, DMSO-d_6): δ (ppm) = 361 (N-15), 297 (N-14), 251 (N-16), 243 (N-8), 52 (N 24). $^{19}F\{^1H\}$ NMR (471 MHz, DMSO-d_6): δ (ppm) = −77.7. $^{195}Pt\{^1H\}$ NMR (107 MHz, DMSO-d_6): δ (ppm) = −3912. HRMS (m/z) $[C_{22}H_{25}ClN_5Pt]^+$: calcd: 589.1441, found: 589.1445.

Synthesis of [PtCl(^{P}L^P)]. A solution of ^{P}LH^P (208 mg, 0.376 mmol, 1.0 equiv.) in 2-ethoxyethanol (12 mL) and water (6 mL) was purged with argon for 30 min. K_2PtCl_4 (156 mg, 0.376 mmol, 1.0 equiv.) was added, and the mixture was stirred at 80 °C under an argon atmosphere for 1 d. The solvent was removed under vacuum and the crude product purified by column chromatography (SiO_2, CH_2Cl_2 : CH_3OH, 100 : 4). The product was obtained as a yellow solid. Yield: 49% (143 mg, 0.183 mmol). ^1H NMR (400 MHz, CD_2Cl_2): δ (ppm) = 8.33 (s, 1H, H-17), 7.39 (t, J = 7.9 Hz, 1H, H-11), 7.17 (d, J = 2.7 Hz, 1H, H-1), 7.12 (d, J = 8.5 Hz, 1H, H-5), 7.03 (d, J = 8.3 Hz, 1H, H-12), 6.93 (d, J = 7.9 Hz, 1H, H-10), 6.65 (dd, J = 8.5, J = 2.7 Hz, 1H, H-4), 4.75 (dt, $^3J_{H,P}$ = 12.5, J = 7.7 Hz, 2H, H-18), 4.38 (d, $^2J_{H,P}$ = 9.6 Hz, 2H, H-23), 4.30–4.20 (m, 4H, H-25), 4.18–4.05 (m, 4H, H-21), 2.57 (dt, $^2J_{H,P}$ = 18.5, J 7.7 Hz, 1H, H-19), 1.39 (t, J = 7.1 Hz, 6H, H-22), 1.33 (t, J = 7.1 Hz, 6H, H-26). $^{13}C\{^1H\}$ NMR (101 MHz, CD_2Cl_2): δ (ppm) = 165.1 (C-7), 160.1 (C-3), 150.0 (C-13), 147.9 (C-9), 142.8 (C-1), 140.2 (C-6), 139.0 (C-11), 126.1 (C-5), 125.8 (C-17), 118.2 (C-2), 116.6 (C-12), 116.3 (C-10), 111.1 (C-4), 63.3, (d, $^3J_{C,P}$ = 6.4 Hz, C-25) 62.2 (d, $^1J_{C,P}$ = 141.4 Hz, C-23), 47.3 (d, $^2J_{C,P}$ = 1.3 Hz, C-18), 26.8 (d, $^1J_{C,P}$ = 141.0 Hz, C-19), 16.8 (d, $^3J_{H,P}$ = 5.8 Hz, C-26), 16.7 (d, $^3J_{H,P}$ = 6.0 Hz, C-22). $^{15}N\{^1H\}$ NMR (41 MHz, CD_2Cl_2): δ (ppm) = 357 (N-15), 301 (N-14), 247 (N-16), 220 (N-8). $^{31}P\{^1H\}$ NMR (162 MHz, CD_2Cl_2): δ (ppm) = 24.9 (P-20), 19.0 (P-24). $^{195}Pt\{^1H\}$ NMR (86 MHz, CD_2Cl_2): δ (ppm) = −3477. HRMS (m/z) $[C_{24}H_{33}N_4O_7P_2ClPt + Na]^+$: calcd: 804.1055, found: 804.1060. Elem. Anal. for $C_{24}H_{33}N_4O_7P_2ClPt$ (%) calcd: C 36.9, H 4.3, N 7.2, found: C 36.2, H 4.5, N 6.8. Single crystals for X-ray structure analysis were obtained by slow diffusion of diethyl ether into a concentrated solution of the complex in DMF.

Synthesis of [Pt(A)(^{P}L^P)]. The general procedure for the synthesis of complexes with auxiliary ligand A was applied to [PtCl(^{P}L^P)] (330 mg, 0.422 mmol, 1.0 equiv.), and the crude product was purified by column chromatography (SiO_2, CH_2Cl_2 : CH_3OH, 100 : 5). The product was obtained as a yellow solid. Yield: 21% (75 mg, 88 μmol). ^1H NMR (400 MHz, CD_2Cl_2): δ (ppm) = 8.39 (s, 1H, H-17), 7.58 (d, J = 2.7 Hz, 1H, H-2), 7.53 (t, J = 7.9 Hz, 1H, H-11), 7.50–7.45 (m, 2H, H-30), 7.32–7.25 (m, 3H, H-31, H-5), 7.23 (d, J = 8.3 Hz, 1H, H-12), 7.21–7.15 (m, 2H, H-32, H-10), 6.66 (dd, J = 8.5 Hz, J = 2.7 Hz, 1H, H-4), 4.75 (t, J = 7.5 Hz, 2H, H-18), 4.36 (d, $^2J_{H,P}$ = 9.7 Hz, 2H, H-23), 4.26–4.15 (m, 4H, H-25), 4.14–3.98 (m, 4H, H-21), 2.51 (dt, $^2J_{H,P}$ = 18.4 Hz, J = 6.8 Hz, 2H, H-19), 1.35 (t, J = 7.1 Hz, 6H, H-26), 1.27 (t, J = 7.1 Hz, 6H, H-22). $^{13}C\{^1H\}$ NMR (101 MHz, CD_2Cl_2): δ (ppm) = 164.2 (C-7), 160.6 (C-3), 151.9 (C-13), 147.7 (C-9), 142.7 (C-1), 140.7 (C-6), 139.6 (C-11), 131.9 (C-30), 129.2 (C-29), 128.5 (C-31), 126.3 (C-5), 125.6 (C-17), 125.5 (C-32), 122.3 (C-2), 117.0 (C-12), 116.3 (C-10), 110.7 (C-4), 105.2 (C-28), 102.6 (C-27), 63.3 (d, $^3J_{C,P}$ = 6.4 Hz, C-25), 62.7 (d, $^3J_{C,P}$ = 6.5 Hz, C-21), 62.2 (d, $^1J_{C,P}$ = 169.5 Hz, C-23), 47.2 (C-18), 26.9 (d, $^1J_{C,P}$ = 141.4 Hz, C-19), 16.7 (d, $^3J_{C,P}$ = 5.7 Hz, C-26),

16.6 (d, $^{3}J_{C,P}$ = 5.9 Hz, C-22). $^{15}N\{^{1}H\}$ NMR (41 MHz, CD_2Cl_2): δ (ppm) = 359 (N-15), 298 (N-14), 246 (N-16), 242 (N-8). $^{31}P\{^{1}H\}$ NMR (162 MHz, CD_2Cl_2): δ (ppm) = 24.8 (P-20), 18.9 (P-24). $^{195}Pt\{^{1}H\}$ NMR (86 MHz, CD_2Cl_2): δ (ppm) = −3863. HRMS (*m*/*z*) $[C_{32}H_{38}N_4O_7P_2Pt + H]^+$: calcd: 848.1936, found: 848.1909. Elem. Anal. for $C_{32}H_{38}N_4O_7P_2Pt$ (%) calcd: C 45.3, H 4.5, N 6.6, found: C 44.9, H 4.8, N 6.4.

Synthesis of [Pt(B)(^{P}L^{P})]OTf. The general procedure for the synthesis of complexes with auxiliary ligand B was applied to [PtCl(^{P}L^{P})] (150 mg, 0.192 mmol). The complex was isolated as an orange solid. Yield: 36% (68 mg, 68 μmol). ^{1}H NMR (400 MHz, DMSO-d_6): δ (ppm) = 9.03 (s, 1H, H-17), 8.01 (t, *J* = 8.0 Hz, 1H, H-11), 7.76 (d, *J* = 8.1 Hz, 1H, H-12), 7.69–7.63 (m, 1H, H-10) (s, 1H, H-10), 7.55 (d, *J* = 8.4 Hz, 1H, H-5), 7.17 (d, *J* = 2.7 Hz, 1H, H-2), 6.75 (dd, *J* = 8.6 Hz, 2.7 Hz, 1H, H-4), 4.73–4.61 (m, 2H, H-18), 4.48–4.38 (m, 4H, H-23), 4.21–4.08 (m, 4H, H-25), 4.06–3.95 (m, 4H, H-21), 3.16 (s, 9H, H-31), 2.60–2.51 (m, 2H, H-19), 1.28 (t, *J* = 7.0 Hz, 6H, H-26), 1.20 (t, *J* = 7.0 Hz, 6H, H-22). $^{13}C\{^{1}H\}$ NMR (101 MHz, DMSO-d_6): δ (ppm) = 163.2 (C-7), 159.9 (C-3), 150.2 (C-13), 146.9 (C-9), 141.8 (C-1), 140.8 (C-11), 140.0 (C-6), 126.6 (C-5), 126.2 (C-17), 123.1 (C-2), 117.3 (C-12), 116.2 (C-10), 108.8 (C-4), 105.2 (C-27), 89.3 (C-28), 62.1 (C-25), 61.4 (C-21), 60.9 (C-23), 59.6 (C-29), 51.0 (C-31), 46.2 (C-18), 25.0 (C-19), 16.2 (C-26), 16.0 (C-22). $^{15}N\{^{1}H\}$ NMR (41 MHz, DMSO-d_6): δ (ppm) = 250 (N-16), 53 (N-30). $^{19}F\{^{1}H\}$ NMR (376 MHz, DMSO-d_6): δ (ppm) = −77.7. $^{31}P\{^{1}H\}$ NMR (162 MHz, DMSO-d_6): δ (ppm) = 25.9 (P-20), 19.7 (P-24). $^{195}Pt\{^{1}H\}$ NMR (86 MHz, DMSO-d_6): δ (ppm) = −3894. HRMS (*m*/*z*) $[C_{30}H_{44}N_5O_7P_2Pt]^+$: calcd: 843.2358, found: 843.2374.

Synthesis of [PtCl(^{OH}L^{OH})]. A solution of ^{OH}LH^{OH} (250 mg, 0.705 mmol, 1.0 equiv.) in 2-ethoxyethanol (5 mL) and water (5 mL) was purged with argon for 30 min. K_2PtCl_4 (293 mg, 0.706 mmol, 1.0 equiv.) was added, and the mixture was stirred at 80 °C under an argon atmosphere for 1 d. The precipitate was filtered, washed with water, ethanol, and diethyl ether, and dried under vacuum. The complex was obtained as a yellow solid. Yield: 57% (234 mg, 0.401 mmol). ^{1}H NMR (500 MHz, DMF-d_7): δ (ppm) = 9.14 (s, 1H, H-17), 8.05–7.98 (m, 1H, H-11), 7.75–7.69 (m, 2H, H-10, H-12), 7.56 (d, *J* = 8.5 Hz, 1H, H-5), 7.30 (d, $^{3}J_{H,Pt}$ = 51 Hz, *J* = 2.6 Hz, 1H, H-2), 6.69 (dd, *J* = 8.6, *J* = 2.6 Hz, 1H, H-4), 4.82 (t, *J* = 5.1 Hz, 1H, H-21), 4.72 (t, *J* = 7.1 Hz, 2H, H-18), 4.62 (t, *J* = 5.3 Hz, 1H, H-25), 4.14 (t, *J* = 6.3 Hz, 2H, H-22), 3.71 (q, *J* = 5.9 Hz, 2H, H-24), 3.63 (q, *J* = 5.6 Hz, 2H, H-20), 2.21 (p, *J* = 6.5 Hz, 2H, H-19), 1.97 (p, *J* = 6.3 Hz, 2H, H-23). $^{13}C\{^{1}H\}$ NMR (126 MHz, DMF-d_7): δ (ppm) = 166.4 (C-7), 161.2 (C-3), 150.4 (C-13), 148.9 (C-9), 143.1 ($^{1}J_{C,Pt}$ = 1117 Hz, C-1), 140.7 (C-11), 139.9 (C-6), 127.3 ($^{3}J_{C,Pt}$ = 49 Hz, C-5), 126.9 (C-17), 120.1 ($^{2}J_{C,Pt}$ = 56 Hz, C-2), 117.7 ($^{3}J_{C,Pt}$ = 46 Hz, C-12), 116.9 ($^{3}J_{C,Pt}$ = 22 Hz, C-10), 110.7 (C-4), 65.4 (C-22), 58.8 (C-20), 58.8 (C-24), 50.3 (C-18), 33.5 (C-23), 33.4 (C-19). $^{15}N\{^{1}H\}$ NMR (51 MHz, DMF-d_7): δ (ppm) = 361 (N-15), 301 (N-14), 252 (N-16), 219 (N-8). $^{195}Pt\{^{1}H\}$ NMR (107 MHz, DMF-d_7): δ (ppm) = −3488. HRMS (*m*/*z*) $[C_{19}H_{21}ClN_4O_3Pt - H]^-$: calcd: 582.0883, found: 582.0860. Elem. Anal. for $C_{19}H_{21}ClN_4O_3Pt$ (%) calcd: C 39.0, H 3.6, N 9.6, found: C 38.6, H 3.8, N 9.4. Single crystals for X-ray structure analysis were obtained by slow diffusion of diethyl ether into a concentrated solution of the complex in *N*,*N* dimethylformamide.

Synthesis of [Pt(A)(^{OH}L^{OH})]. The general procedure for the synthesis of complexes with auxiliary ligand A was applied to [PtCl(^{OH}L^{OH})] (210 mg, 0.360 mmol, 1.0 equiv.), the crude product was purified by column chromatography (Al_2O_3, CH_2Cl_2 : CH_3OH, 100 : 3). The product was obtained as a yellow solid. Yield: 24% (56 mg, 86 μmol). ^{1}H NMR (400 MHz, DMSO-d_6): δ (ppm) = 9.08 (s, 1H, H-17), 8.00 (t, *J* = 8.0 Hz, 1H, H-11), 7.75 (d, *J* = 8.3 Hz, 1H, H-12), 7.71 (d, *J* = 7.7 Hz, 1H, H-10), 7.56 (d, *J* = 8.6 Hz, 1H, H-5), 7.43 (d, *J* = 2.7 Hz, 1H, H-2), 7.35–7.22 (m, 4H, H-30, H-29), 7.19–7.10 (m, 1H, H-31), 6.63 (dd, *J* = 8.5, 2.7 Hz, 1H, H-4), 4.76 (s, 1H, H-21), 4.61 (t, *J* = 7.1 Hz, 2H, H-18), 4.55 (s, 1H, H-25), 4.07 (t, *J* = 6.4 Hz, 2H, H-22), 3.60–3.52 (m, 2H, H-24), 3.48 (t, *J* = 5.9 Hz, 2H, H-20), 2.16–2.04 (m, 2H, H-19), 1.92–1.82 (m, 2H, H-23). $^{13}C\{^{1}H\}$ NMR (101 MHz, DMSO-d_6): δ (ppm) = 163.6 (C-7), 160.1 (C-3), 150.7 (C-13), 147.2 (C-9), 141.8 (C-1), 140.4 (C-11), 138.9 (C-6), 130.8 (C-29), 128.9 (C-28), 128.0 (C-30), 126.5 (C-5), 125.9 (C-17), 124.7 (C-31), 122.6 (C-2), 116.8 (C-12), 115.8 (C-10), 109.3 (C-4), 104.9 (C-26), 103.9 (C-27), 64.2 (C-22), 57.2 (C-24, C-20), 48.9 (C-18), 32.1 (C-23, C-19). $^{15}N\{^{1}H\}$ NMR (41 MHz, DMSO-d_6): δ (ppm) = 361 (N-15), 297 (N-14), 253 (N-16), 242 (N-8). $^{195}Pt\{^{1}H\}$ NMR (86 MHz, DMSO-d_6): δ (ppm) = −3884. HRMS (*m*/*z*) $[C_{27}H_{26}N_4O_3Pt + H]^+$: calcd: 650.1725, found: 650.1722. Elem. Anal. for $C_{27}H_{26}N_4O_3Pt$ (%) calcd: C 49.9, H 4.0, N 8.6, found: C 49.9, H 4.4, N 8.2.

Synthesis of [Pt(B)(^{OH}L^{OH})]OTf. The general procedure for the synthesis of complexes with auxiliary ligand B was applied to [PtCl(^{OH}L^{OH})] (200 mg, 0.343 mmol). The complex was isolated as an orange solid. Yield: 52% (141 mg, 0.177 mmol). ^{1}H NMR (400 MHz, D_2O, pD 8.2): δ (ppm) = 8.19 (s, 1H, H-17), 7.46 (t, *J* = 7.9 Hz, 1H, H-11), 7.15 (d, *J* = 8.1 Hz, 1H, H-12), 7.11 (d, *J* = 8.6 Hz, 1H, H-5), 7.04 (d, *J* = 7.7 Hz, 1H, H-10), 6.75 (d, *J* = 2.6 Hz, 1H, H-2), 6.52 (dd, *J* = 8.5 Hz, *J* = 2.7 Hz, 1H, H-4), 4.39 (t, *J* = 7.2 Hz, 2H, H-18), 4.31 (s, 2H, H-28), 4.09 (t, *J* = 6.4 Hz, 2H, H-22), 3.82 (t, *J* = 6.3 Hz, 2H, H-24), 3.67 (t, *J* = 6.1 Hz, 2H, H-20), 3.24 (s, 9H, H-30), 2.18–2.10 (m, 2H, H-19), 2.09–1.97 (m, 2H, H-23). $^{13}C\{^{1}H\}$ NMR (101 MHz, D_2O, pD 8.2): δ (ppm) = 165.5 (C-7), 162.0 (C-3), 154.0 (C-13), 149.5 (C-9), 143.5 (C-1), 142.9 (C-6), 142.7 (C-11), 129.2 (C-5), 127.4 (C-17), 124.7 (C-2), 119.9 (C-12), 118.9 (C-10), 112.2 (C-4), 107.7 (C-26), 92.6 (C-27), 67.7 (C-22), 62.5 (C-28), 61.1 (C-24), 60.8 (C-20), 54.5 (C-30), 51.6 (C-18), 34.0 (C-19), 33.8 (C-23). $^{15}N\{^{1}H\}$ NMR (41 MHz, D_2O, pD 8.2): δ (ppm) = 355 (N-15), 295 (N-14), 250 (N-16), 239 (N-8), 52 (N 29). $^{19}F\{^{1}H\}$ NMR (376 MHz, D_2O, pD 8.2): δ (ppm) = −78.8. $^{195}Pt\{^{1}H\}$ NMR (86 MHz, D_2O, pD 8.2): δ (ppm) = −3871. HRMS (*m*/*z*) $[C_{25}H_{32}N_5O_3Pt + H]^+$: calcd: 645.2147, found: 645.2161.

Synthesis of [PtCl(^{Cl}L^{Cl})]. A solution of ^{Cl}LH^{Cl} (250 mg, 0.639 mmol, 1.0 equiv.) in acetic acid (20 mL) was purged with argon for 30 min. K_2PtCl_4 (265 mg, 0.643 mmol, 1.0 equiv.) was added and the mixture was stirred at 120 °C under an argon atmosphere for 3 d. The precipitate was filtered, washed with water, ethanol, and diethyl ether, and dried under vacuum. The complex was obtained as a yellow solid. Yield:

43% (172 mg, 0.277 mmol). ^{1}H NMR (500 MHz, DMF-d_7): δ (ppm) = 9.16 (s, 1H, H-17), 7.98 (t, J = 8.0 Hz, 1H, H-11), 7.70 (td, J = 8.1, 1.0 Hz, 2H, H-10, H-12), 7.56 (d, J = 8.6 Hz, 1H, H-5), 7.29 (d, J = 2.6 Hz, 1H, H-2), 6.71 (dd, J = 8.5, 2.7 Hz, 1H, H-4), 4.80 (t, J = 6.9 Hz, 2H, H-18), 4.19 (t, J = 6.0 Hz, 2H, H-21), 3.87 (t, J = 6.5 Hz, 2H, H-23), 3.84 (t, J = 6.4 Hz, 2H, H-20), 2.54 (p, J = 6.7 Hz, 2H, H-19), 2.26 (p, J = 6.3 Hz, 2H, H-22). ^{13}C{^{1}H} NMR (126 MHz, DMF-d_7): δ (ppm) = 166.0 (C-7), 160.6 (C-3), 150.3 (C-13), 148.6 (C-9), 142.9 (C-1), 140.4 (C-11), 140.1 (C-6), 127.1 (C-5), 126.9 (C-17), 119.9 (C-2), 117.6 (C-12), 116.8 (C-10), 110.5 (C-4), 64.9 (C-21), 50.1 (C-18), 42.6 (C-23), 42.4 (C-20), 32.9 (C-19. C-22). ^{15}N{^{1}H} NMR (51 MHz, DMF-d_7): δ (ppm) = 360 (N-15), 302 (N-14), 250 (N-16), 219 (N-8). ^{195}Pt{^{1}H} NMR (202 MHz, DMF-d_7): δ (ppm) = −3485. HRMS (m/z) $[C_{19}H_{19}Cl_3N_4OPt + H]^+$: calcd: 620.0350, found: 620.0337. Elem. Anal. for $C_{19}H_{19}Cl_3N_4OPt$ (%) calcd: C 36.8, H 3.1, N 9.0, found: C 36.8 H 3.2, N 9.0.

Synthesis of [Pt(A)(^{Cl}L^{Cl})]. The general procedure for the synthesis of complexes with auxiliary ligand A was applied to [PtCl(^{Cl}L^{Cl})] (300 mg, 0.483 mmol), and the crude product was purified by column chromatography (Al_2O_3, CH_2Cl_2 : CH_3OH, 100 : 0.3). The product was obtained as a yellow solid. Yield: 43% (143 mg, 0.203 mmol). ^{1}H NMR (500 MHz, CD_2Cl_2): δ (ppm) = 8.21 (s, 1H, H-17), 7.50 (d, J = 2.6 Hz, 1H, H-2), 7.48–7.41 (m, 2H, H-27), 7.33–7.25 (m, 3H, H-28, H-11), 7.23–7.16 (m, 2H, H-29, H-5), 7.06 (d, J = 8.1 Hz, 1H, H-10), 6.96 (d, J = 7.7 Hz, 1H, H-12), 6.60 (dd, J = 8.5, 2.7 Hz, 1H, H-4), 4.65 (t, J = 7.1 Hz, 2H, H-18), 4.20 (t, J = 5.9 Hz, 2H, H-21), 3.77 (t, J = 6.4 Hz, 2H, H-23), 3.52 (t, J = 6.1 Hz, 2H, H-20), 2.43 (p, J = 6.6 Hz, 2H, H-19), 2.25 (p, J = 6.2 Hz, 2H, H-22). ^{13}C{^{1}H} NMR (126 MHz, CD_2Cl_2): δ (ppm) = 164.1 (C-7), 160.9 (C-3), 151.6 (C-13), 147.3 (C-9), 142.3 (C-1), 139.7 (C-6), 139.1 (C-11), 131.8 (C-27), 129.2 (C-26), 128.6 (C-28), 126.4 (C-5), 125.7 (C-17), 125.6 (C-29), 123.0 (C-2), 116.5 (C-10), 116.2 (C-12), 110.3 (C-4), 105.1 (C-25), 102.8 (C-24), 64.6 (C-21), 50.0 (C-18), 42.3 (C-23), 41.8 (C-20), 32.7 (C-22), 32.3 (C-19). ^{15}N{^{1}H} NMR (51 MHz, CD_2Cl_2): δ (ppm) = 358 (N-15), 297 (N-14), 247 (N-16), 241 (N-8). ^{195}Pt{^{1}H} NMR (107 MHz, CD_2Cl_2) δ (ppm) = −3852. HRMS (m/z) $[C_{27}H_{24}Cl_2N_4OPt + H]^+$: calcd: 686.1048, found: 686.1043. Elem. Anal. for $C_{27}H_{24}Cl_2N_4OPt$ (%) calcd: C 47.2, H 3.5, N 8.2, found: C 47.5, H 3.9, N 8.2.

Synthesis of [Pt(B)(^{Cl}L^{Cl})]OTf. The general procedure for the synthesis of complexes with auxiliary ligand B was applied to [PtCl(^{Cl}L^{Cl})] (200 mg, 0.322 mmol). The complex was isolated as an orange solid. Yield: 46% (124 mg, 0.149 mmol). ^{1}H NMR (400 MHz, DMSO-d_6): δ (ppm) = 9.06 (s, 1H, H-17), 8.02 (t, J = 8.0 Hz, 1H, H-11), 7.76 (d, J = 8.2 Hz, 1H, H-12), 7.69 (d, J = 7.7 Hz, 1H, H-10), 7.56 (d, J = 8.5 Hz, 1H, H-5), 7.17 (d, J = 2.6 Hz, 1H, H-2), 6.67 (dd, J = 8.5 Hz, J = 2.7 Hz, 1H, H-4), 4.65 (t, J = 6.8 Hz, 2H, H-18), 4.42 (s, 2H, H-26), 4.10 (t, J = 6.0 Hz, 2H, H-21), 3.81 (t, J = 6.4 Hz, 2H, H-23), 3.73 (t, J = 6.3 Hz, 2H, H-20), 3.16 (s, 9H, H-28), 2.45–2.34 (m, 2H, H-19), 2.25–2.13 (m, 2H, H-22). ^{13}C{^{1}H} NMR (101 MHz, DMSO-d_6): δ (ppm) = 163.5 (C-7), 159.9 (C-3), 150.6 (C-13), 147.2 (C-9), 141.8 (C-1), 140.8 (C-11), 139.3 (C-6), 126.7 (C-5), 126.2 (C-17), 122.9 (C-2), 117.1 (C-12), 116.1 (C-10), 109.4 (C-4, C-24), 89.3 (C-25), 63.9 (C-21), 59.4 (C-26), 50.9 (C-28), 48.9 (C-18), 41.9 (C-23), 41.8 (C-20), 31.6 (C-19, C-22). ^{15}N{^{1}H} NMR (41 MHz, DMSO-d_6): δ (ppm) = 360 (N-15), 296 (N-14), 251 (N-16), 240 (N-8), 53 (N-30). ^{19}F{^{1}H} NMR (376 MHz, DMSO-d_6): δ (ppm) = −77.7. ^{195}Pt{^{1}H} NMR (86 MHz, DMSO-d_6): δ (ppm) = −3898. HRMS (m/z) $[C_{25}H_{30}Cl_2N_5OPt]^+$: calcd: 681.1470, found: 681.1481.

Synthesis of [PtCl(^{M}L^{M})]. A solution of ^{M}LH^{M} (150 mg, 0.304 mmol, 1.0 equiv.) in acetic acid (20 mL) was purged with argon for 30 min. K_2PtCl_4 (126 mg, 0.304 mmol, 1.0 equiv.) was added, and the mixture was stirred at 120 °C under an argon atmosphere for 3 d. Diethyl ether (15 mL) was added to the solution at room temperature. The resulting precipitate was filtered, redissolved in CH_2Cl_2 (20 mL), and saturated aqueous solution of $NaHCO_3$ (20 mL) was added. The aqueous phase was washed three times with CH_2Cl_2 and the combined organic layers dried ($MgSO_4$). The residue was purified by column chromatography (SiO_2, CH_2Cl_2 : CH_3OH, 100 : 7). The complex was obtained as a yellow solid. Yield: 29% (63 mg, 87 μmol). ^{1}H NMR (400 MHz, DMF-d_7): δ (ppm) = 9.25 (s, 1H, H-17), 8.08–8.01 (m, 1H, H-11), 7.80–7.72 (m, 2H, H-10, H-12), 7.59 (d, J = 8.6 Hz, 1H, H-5), 7.27 (d, J = 2.6 Hz, 1H, H-2), 6.70 (dd, J = 8.5, J = 2.6 Hz, 1H, H-4), 4.74 (t, J = 6.9 Hz, 2H, H-18), 4.14 (t, J = 6.2 Hz, 2H, H-24), 3.87 (br, 4H, H-29), 3.70 (s, 4H, H-23), 2.97 (s, 2H, H-26), 2.59 (br, 10H, H-20, H-22, H-28), 2.32 (br, 2H, H-19), 2.21 (br, 2H, H-25). ^{13}C{^{1}H} NMR (101 MHz, DMF-d_7): δ (ppm) = 166.2 (C-7), 160.7 (C-3), 150.2 (C-13), 148.8 (C-9), 142.9 (C-1), 140.5 (C-11), 140.0 (C-6), 127.1 (C-5), 126.9 (C-17), 120.1 (C-2), 117.6 (C-12), 116.8 (C-10), 110.3 (C-4), 66.5 (C-23), 65.6 (C-29), 65.4 (C-24), 55.3 (C-20, C-26), 53.7 (C-22), 53.2 (C-28), 50.8 (C-18), 26.2 (C-19), 25.4 (C-25). ^{15}N{^{1}H} NMR (41 MHz, DMF-d_7): δ (ppm) = 301 (N-14), 251 (N-16), 220 (N-8). ^{195}Pt{^{1}H} NMR (107 MHz, DMF-d_7): δ (ppm) = 3486. HRMS (m/z) $[C_{27}H_{35}ClN_6O_3Pt + H]^+$: calcd: 722.2180, found: 722.2180. Elem. Anal. for $C_{27}H_{35}ClN_6O_3Pt$ (%) calcd: C 44.9, H 4.9, N 11.6, found: C 44.8 H 4.9, N 11.4.

Synthesis of [Pt(A)(^{M}L^{M})]. The general procedure for the synthesis of complexes with auxiliary ligand A was applied to [PtCl(^{M}L^{M})] (60 mg, 83 μmol, 1.0 equiv.), and the crude product was purified by column chromatography (SiO_2, CH_2Cl_2 : CH_3OH, 100 : 7). The product was obtained as a yellow solid. Yield: 43% (28 mg, 36 μmol). ^{1}H NMR (400 MHz, CD_2Cl_2): δ (ppm) = 8.23 (s, 1H, H-17), 7.56 (d, J = 2.7 Hz, 1H, H-2), 7.52–7.43 (m, 3H, H-11, H-33), 7.33–7.26 (m, 3H, H-5, H-34), 7.24–7.14 (m, 2H, H-12, H-35), 7.09 (d, J = 7.7 Hz, 1H, H-10), 6.62 (dd, J = 8.5, J = 2.7 Hz, 1H, H-4), 4.58 (t, J = 7.2 Hz, 2H, H-18), 4.12 (t, J = 6.4 Hz, 2H, H-24), 3.65 (t, J = 4.7 Hz, 4H, H-29), 3.61 (t, J = 4.7 Hz, 4H, H-23), 2.49 (t, J = 7.2 Hz, 2H, H-26), 2.44–2.38 (m, 4H, H-28), 2.37–2.27 (m, 6H, H-20, H-22), 2.14 (p, J = 6.8 Hz, 2H, H-19), 1.95 (p, J = 6.7 Hz, 2H, H-25). ^{13}C{^{1}H} NMR (101 MHz, CD_2Cl_2): δ (ppm) = 164.7 ($^{2}J_{C,Pt}$ = 97 Hz, C-7), 161.4 ($^{3}J_{C,Pt}$ = 91 Hz, C-3), 151.5 ($^{2}J_{C,Pt}$ = 41 Hz, C-13), 147.6 (C-9), 142.5 ($^{1}J_{C,Pt}$ = 1124 Hz, C-1), 139.5 (C-11), 139.4 (C-6), 131.9 (C-33), 129.4 (C-32), 128.5 (C-33), 126.4 ($^{3}J_{C,Pt}$ = 52 Hz, C-5), 125.5 (C-35), 125.2 (C-17), 123.0 ($^{2}J_{C,Pt}$ = 107 Hz, C-2), 116.6 (C-12), 115.7 (C-10), 110.6 (C-4), 105.2 ($^{2}J_{C,Pt}$ = 407 Hz,

C-31), 102.9 ($^1J_{C,Pt}$ = 1530 Hz, C-30), 67.3 (C-29), 67.2 (C-23), 66.4 (C-24), 55.8 (C-26), 55.2 (C-20), 54.2 (C-28), 53.9 (C 22), 50.9 (C-18), 26.9 (C-25) 26.8 (C-19). $^{15}N\{^1H\}$ NMR (41 MHz, CD_2Cl_2): δ (ppm) = 360 (N-15), 297 (N-14), 250 (N-16), 243 (N-8), 44 (N-27), 42 (N-21). $^{195}Pt\{^1H\}$ NMR (86 MHz, CD_2Cl_2): δ (ppm) = −3862. HRMS (*m*/*z*) $[C_{35}H_{40}N_6O_3Pt + H]^+$: calcd: 788.2882, found: 788.2889. Elem. Anal. for $C_{35}H_{40}N_6O_3Pt$ (%) calcd: C 53.4, H 5.1, N 10.7, found: C 53.1, H 5.3, N 10.5.

Synthesis of [Pt(B)(^{M}L^{M})]OTf. The general procedure for the synthesis of complexes with auxiliary ligand B was applied to [PtCl(^{M}L^{M})] (136 mg, 0.188 mmol). The complex was isolated as an orange solid. Yield: 22% (39 mg, 42 μmol). ^1H NMR (400 MHz, DMSO-d_6): δ (ppm) = 9.07 (s, 1H, H-17), 8.03 (t, *J* = 8.0 Hz, 1H, H-11), 7.78 (d, *J* = 8.2 Hz, 1H, H-12), 7.72 (d, *J* = 7.7 Hz, 1H, H-10), 7.58 (d, *J* = 8.6 Hz, 1H, H-5), 7.17 (d, *J* = 2.6 Hz, 1H, H-2), 6.64 (dd, *J* = 8.5 Hz, 2.6 Hz, 1H, H-4), 4.57 (t, *J* = 6.9 Hz, 2H, H-18), 4.39 (s, 2H, H-32), 4.00 (t, *J* = 6.3 Hz, 2H, H-24), 3.58 (t, *J* = 4.6 Hz, 4H, H-23), 3.54 (t, *J* = 4.6 Hz, 4H, H-29), 3.15 (s, 9H, H-34), 2.47–2.28 (m, 12H, H-20, H-22, H-26, H-28), 2.15–2.01 (m, 2H, H-19), 1.95–1.84 (m, 2H, H-25). $^{13}C\{^1H\}$ NMR (126 MHz, DMSO-d_6): δ (ppm) = 163.6 (C-7), 160.2 (C-3), 150.5 (C-13), 147.3 (C-9), 141.6 (C-1), 140.8 (C-11), 139.1 (C-6), 126.8 (C-5), 126.2 (C-17), 122.7 (C-2), 121.86, 117.9 (C-12), 115.9 (C-10), 109.5 (C-5), 104.7 (C-30), 89.3 (C-31), 66.0 (C-23, C-29), 65.4 (C-24), 59.1 (C-32), 54.7 (C-26), 54.6 (C-20), 53.3 (C-22), 53.0 (C-28), 50.8 (C-34), 45.0 (C-18), 25.8 (C-25), 25.7 (C-19). $^{15}N\{^1H\}$ NMR (41 MHz, DMSO-d_6): δ (ppm) = 361 (N-15), 295 (N-14), 253 (N-16), 240 (N-8), 43 (N 27). $^{19}F\{^1H\}$ NMR (376 MHz, DMSO-d_6): δ (ppm) = −77.7. $^{195}Pt\{^1H\}$ NMR (107 MHz, DMSO- d_6): δ (ppm) = −3901. HRMS (*m*/*z*) $[C_{33}H_{46}N_7O_3Pt]^+$: calcd: 783.3304, found: 788.3316.

Conclusions

By varying the substitution pattern of a tridentate N^N^C ligand as well as the identity of a monodentate ancillary ligand, 16 new luminescent platinum(II) complexes for the selective binding of guanine quadruplexes were designed and synthesized. Based on DFT studies, the ability of the complexes to aggregate was predicted computationally and then (mostly) confirmed experimentally in aqueous medium. As expected, complexes bearing positively charged substituents were less likely to aggregate in solution. Four guanine quadruplexes that are currently being discussed as potential therapeutic agents were exemplarily chosen for the interaction studies.

Cryo-ESI mass spectrometry indicates two possible binding stoichiometries of G4 DNA per complex, namely 1 : 1 and 1 : 2, with the former being more prominent. A phosphorescence turn-on is observed upon the addition of G4 DNA to most of the complexes, with the complexes bearing a phosphate ester substituent being a notable exception (except for [Pt(B)(^{P}L)]OTf). Interestingly, the presence of *c-kit* hardly affects the luminescence of the Pt(II) complexes, whereas *c-myc*22 particularly affects that of complexes with auxiliary ligand A. The luminescence data also suggest a significant interaction of [Pt(A)(^{M}L^{M})] (with its two morpholino-group containing substituents) with all oligonucleotides under investigation. This correlates well with the use of morpholine as a protonatable group in earlier studies on G4 binders.[22] As the overall increase in luminescence depends on the nature of the G4 quadruplex, some selectivity towards the different G4 topologies can be anticipated.

CD spectroscopic studies do not indicate major structural changes of the G4 DNA upon addition of complexes with luminescence turn-on. However, in *c-myc22* and *bcl2*-mid a structural change does occur (based on CD spectra) in the presence of [Pt(B)(^{M}L)]OTf and [Pt(B)(^{P}L^{P})]OTf, respectively, even though this change is neither accompanied by a stabilizing effect nor by a significant change in luminescence. In the case of *bcl2*-mid and [Pt(B)(^{P}L^{P})]OTf, a complete unfolding of the G4 DNA is proposed.

[Pt(A)(^{M}L^{M})] and [Pt(B)(^{OH}L)]OTf are the two complexes inducing the greatest G4 DNA stabilization (based on ΔT_m for FAM-*bcl2*-mid-DABCYL). However, there appears to be no particular selectivity of these two complexes for any of the four G4 DNA sequences under investigation.

In general, the affinity towards G4 DNA and the selectivity for targeting G4 DNA over double-stranded DNA depends on the functionalization of both the tridentate ligand and the ancillary ligand. Complexes with one or two protonatable/polar substituents appear to interact best with G4 DNA, as can be seen from the data obtained for the morpholino- and hydroxy-functionalized complexes. This points at the relevance of an electrostatic interaction with the phosphate backbone. Future studies will need to focus on increasing the binding affinity of these water-soluble complexes and on improving their binding selectivity towards G4 DNA over dsDNA.

Author contributions

SK: investigation (syntheses, spectroscopy, experiments), writing – original draft; MH: investigation (calculations, ESI-MS measurements); ML: investigation (X-ray diffraction); AH: investigation (NMR spectroscopy); JL: investigation (lifetime measurements); ART: investigation (spectroscopy, experiments); CAS: supervision; JM: supervision, conceptualization; writing – review & editing.

Data availability

The data supporting this article have been included as part of the ESI.† Crystallographic data for [Pt(A)(^{M}L)], [Pt(A)(^{Cl}L)], [PtCl(^{P}L^{P})], and [PtCl(^{OH}L^{OH})] have been deposited at the CCDC under 2392538–2392541.†

Conflicts of interest

There are no conflicts to declare.

Acknowledgements

Calculations for this publication were performed on the HPC cluster PALMA II of the University of Münster, subsidised by the DFG (INST 211/667-1). We thank Bart Jan Ravoo for access to the ITC instrument and Katharina Ziegler and Bastian Stövesand for an introduction into the instrument. J. M. and C. A. S. thank the DFG for funding (SFB 858, STR 1186/7-2).

References

1 *Quadruplex Nucleic Acids*, ed. S. Neidle and S. Balasubramanian, RSC Publishing, 2006.
2 A. Ambrus, D. Chen, J. Dai, R. A. Jones and D. Yang, *Biochemistry*, 2005, **44**, 2048–2058.
3 D. Rhodes and H. J. Lipps, *Nucleic Acids Res.*, 2015, **43**, 8627–8637.
4 M. L. Bochman, K. Paeschke and V. A. Zakian, *Nat. Rev. Genet.*, 2012, **13**, 770–780.
5 R. C. Monsen, J. O. Trent and J. B. Chaires, *Acc. Chem. Res.*, 2022, **55**, 3242–3252.
6 S. Burge, G. N. Parkinson, P. Hazel, A. K. Todd and S. Neidle, *Nucleic Acids Res.*, 2006, **34**, 5402–5415.
7 D. Yang and K. Okamoto, *Future Med. Chem.*, 2010, **2**, 619–646.
8 R. K. Moyzis, J. M. Buckingham, L. S. Cram, M. Dani, L. L. Deaven, M. D. Jones, J. Meyne, R. L. Ratliff and J.-R. Wu, *Proc. Natl. Acad. Sci. U. S. A.*, 1988, **85**, 6622–6626.
9 M. A. Shammas, *Curr. Opin. Clin. Nutr. Metab. Care*, 2011, **14**, 28–34.
10 N. W. Kim, M. A. Piatyszek, K. R. Prowse, C. B. Harley, M. D. West, P. L. C. Ho, G. M. Coviello, W. E. Wright, S. L. Weinrich and J. W. Shaw, *Science*, 1994, **266**, 2011–2015.
11 M. A. Blasco, *Eur. J. Cell Biol.*, 2003, **82**, 441–446.
12 S. Neidle, *Nat. Rev. Chem.*, 2017, **1**, 0041.
13 T. R. Cech, *Angew. Chem., Int. Ed.*, 2000, **39**, 34–43.
14 A. Siddiqui-Jain, C. L. Grand, D. J. Bearss and L. H. Hurley, *Proc. Natl. Acad. Sci. U. S. A.*, 2002, **99**, 11593–11598.
15 D. Sun and L. H. Hurley, *J. Med. Chem.*, 2009, **52**, 2863–2874.
16 S. Hu, W. Ma, J. Wang, Z. Zhou, Y. Ma, R. Zhang, K. Du, H. Zhang, M. Sun, X. Jiang, H. Tu, X. Tang, X. Yao and P. Chen, *Eur. J. Pharmacol.*, 2022, **915**, 174514.
17 B. R. Vummidi, J. Alzeer and N. W. Luedtke, *ChemBioChem*, 2013, **14**, 540–558.
18 R. Hänsel-Hertsch, M. Di Antonio and S. Balasubramanian, *Nat. Rev. Mol. Cell Biol.*, 2017, **18**, 279–284.
19 U. Chilakamarthi, D. Koteshwar, S. Jinka, N. V. Krishna, K. Sridharan, N. Nagesh and L. Giribabu, *Biochemistry*, 2018, **57**, 6514–6527.
20 L. D'Anna, S. Rubino, C. Pipitone, G. Serio, C. Gentile, A. Palumbo Piccionello, F. Giannici, G. Barone and A. Terenzi, *Dalton Trans.*, 2023, **52**, 2966–2975.
21 A. Arola-Arnal, J. Benet-Buchholz, S. Neidle and R. Vilar, *Inorg. Chem.*, 2008, **47**, 11910–11919.
22 S. N. Georgiades, N. H. A. Karim, K. Suntharalingam and R. Vilar, *Angew. Chem., Int. Ed.*, 2010, **49**, 4020–4034.
23 J. Zegers, M. Peters and B. Albada, *J. Biol. Inorg. Chem.*, 2023, **28**, 117–138.
24 A. E. Engelhart, J. Plavec, Ö. Persil and N. V. Hud, in *Nucleic Acid-Metal Ion Interactions*, ed. N. V. Hud, RSC Publishing, Cambridge, UK, 2009, pp. 118–153.
25 A. Maraval, S. Franco, C. Vialas, G. Pratviel, M. A. Blasco and B. Meunier, *Org. Biomol. Chem.*, 2003, **1**, 921–927.
26 T. Kench, V. Rakers, D. Bouzada, J. Gomez-González, J. Robinson, M. K. Kuimova, M. Vázquez López, M. E. Vázquez and R. Vilar, *Bioconjugate Chem.*, 2023, **34**, 911–921.
27 A. Schmidt, R. Guha, A. Hepp and J. Müller, *J. Inorg. Biochem.*, 2017, **175**, 58–66.
28 V. T. Tran, J. Turek-Herman, M. Ferreira, K. N. Martin, D. Beseiso, B. R. Williams, F. Rosu, V. Gabelica, S. J. Nieter Burgmayer and L. A. Yatsunyk, *J. Inorg. Biochem.*, 2023, **249**, 112388.
29 L. Holden, K. S. Gkika, C. S. Burke, C. Long and T. E. Keyes, *Inorg. Chem.*, 2023, **62**, 2213–2227.
30 C. Kaußler, D. Wragg, C. Schmidt, G. Moreno-Alcántar, C. Jandl, J. Stephan, R. A. Fischer, S. Leoni, A. Casini and R. Bonsignore, *Inorg. Chem.*, 2022, **61**, 20405–20423.
31 J. Weynand, H. Bonnet, F. Loiseau, J.-L. Ravanat, J. Dejeu, E. Defrancq and B. Elias, *Chem. – Eur. J.*, 2019, **25**, 12730–12739.
32 C. J. Castor, J. Mancini, J. Fakhoury, N. Weill, R. Kieltyka, P. Englebienne, N. Avakyan, A. Mittermaier, C. Autexier, N. Moitessier and H. F. Sleiman, *ChemMedChem*, 2012, **7**, 85–94.
33 J. Berrones Reyes, P. S. Sherin, A. Sarkar, M. K. Kuimova and R. Vilar, *Angew. Chem., Int. Ed.*, 2023, **62**, e202310402.
34 M. Saini and T. E. Keyes, *Dalton Trans.*, 2023, **52**, 7787–7791.
35 R. Guha, D. Defayay, A. Hepp and J. Müller, *ChemPlusChem*, 2021, **86**, 662–673.
36 M. Hebenbrock, L. Stegemann, J. Kösters, N. L. Doltsinis, J. Müller and C. A. Strassert, *Dalton Trans.*, 2017, **46**, 3160–3169.
37 M. Hebenbrock, D. González-Abradelo, A. Hepp, J. Meadowcroft, N. Lefringhausen, C. A. Strassert and J. Müller, *Inorg. Chim. Acta*, 2021, **516**, 119988.
38 I. Maisuls, F. Boisten, M. Hebenbrock, J. Alfke, L. Schürmann, B. Jasper-Peter, A. Hepp, M. Esselen, J. Müller and C. A. Strassert, *Inorg. Chem.*, 2022, **61**, 9195–9204.
39 A. Gil-Martínez, A. Hernández, C. Galiana-Roselló, S. López-Molina, J. Ortiz, Á. Sastre-Santos, E. García-España and J. González-García, *J. Biol. Inorg. Chem.*, 2023, **28**, 495–507.
40 X. Xie, O. Reznichenko, L. Chaput, P. Martin, M.-P. Teulade-Fichou and A. Granzhan, *Chem. – Eur. J.*, 2018, **24**, 12638–12651.

41 K. Suntharalingam, A. Łęczkowska, M. A. Furrer, Y. Wu, M. K. Kuimova, B. Therrien, A. J. P. White and R. Vilar, *Chem. – Eur. J.*, 2012, **18**, 16277–16282.
42 A. Shivalingam, M. A. Izquierdo, A. Le Marois, A. Vyšniauskas, K. Suhling, M. K. Kuimova and R. Vilar, *Nat. Commun.*, 2015, **6**, 8178.
43 L.-Y. Liu, W. Liu, K.-N. Wang, B.-C. Zhu, X.-Y. Xia, L.-N. Ji and Z.-W. Mao, *Angew. Chem., Int. Ed.*, 2020, **59**, 9719–9726.
44 B. M. Zeglis, V. C. Pierre and J. K. Barton, *Chem. Commun.*, 2007, 4565–4579.
45 J. Dai, M. Carver, C. Punchihewa, R. A. Jones and D. Yang, *Nucleic Acids Res.*, 2007, **35**, 4927–4940.
46 V. González and L. H. Hurley, *Annu. Rev. Pharmacol. Toxicol.*, 2010, **50**, 111–129.
47 J. Dai, D. Chen, R. A. Jones, L. H. Hurley and D. Yang, *Nucleic Acids Res.*, 2006, **34**, 5133–5144.
48 A. T. Phan, V. Kuryavyi, S. Burge, S. Neidle and D. J. Patel, *J. Am. Chem. Soc.*, 2007, **129**, 4386–4392.
49 E. F. Pettersen, T. D. Goddard, C. C. Huang, G. S. Couch, D. M. Greenblatt, E. C. Meng and T. E. Ferrin, *J. Comput. Chem.*, 2004, **25**, 1605–1612.
50 D. Escher, M. N. Hossain, H.-B. Kraatz and J. Müller, *J. Biol. Inorg. Chem.*, 2021, **26**, 659–666.
51 A. Ouedraogo and J. Lessard, *Can. J. Chem.*, 1991, **69**, 474–480.
52 T. L. J. Huang and D. G. Brewer, *Can. J. Chem.*, 1981, **59**, 1689–1700.
53 M. B. Smith, *March's Advanced Organic Chemistry: Reactions, Mechanisms, and Structure*, Wiley, 8th edn, 2020.
54 J.-Y. Cho, K. Y. Suponitsky, J. Li, T. V. Timofeeva, S. Barlow and S. R. Marder, *J. Organomet. Chem.*, 2005, **690**, 4090–4093.
55 B. Lippert, *Cisplatin – Chemistry and Biochemistry of a Leading Anticancer Drug*, Wiley-VCH and Verlag Helvetica Chimica Acta, Zürich, 1999.
56 A. G. Orpen, L. Brammer, F. H. Allen, O. Kennard, D. G. Watson and R. Taylor, *J. Chem. Soc., Dalton Trans.*, 1989, S1–S83.
57 T. Lu and F. Chen, *J. Comput. Chem.*, 2012, **33**, 580–592.
58 J. S. Murray, T. Brinck, P. Lane, K. Paulsen and P. Politzer, *J. Mol. Struct.:THEOCHEM*, 1994, **307**, 55–64.
59 J. A. G. Williams, A. Beeby, E. S. Davies, J. A. Weinstein and C. Wilson, *Inorg. Chem.*, 2003, **42**, 8609–8611.
60 A. Galstyan, A. R. Naziruddin, C. Cebrián, A. Iordache, C. G. Daniliuc, L. De Cola and C. A. Strassert, *Eur. J. Inorg. Chem.*, 2015, 5822–5831.
61 N. K. Allampally, C.-G. Daniliuc, C. A. Strassert and L. De Cola, *Inorg. Chem.*, 2015, **54**, 1588–1596.
62 C. A. Strassert, C.-H. Chien, M. D. Galvez Lopez, D. Kourkoulos, D. Hertel, K. Meerholz and L. De Cola, *Angew. Chem., Int. Ed.*, 2011, **50**, 946–950.
63 R. del Villar-Guerra, J. O. Trent and J. B. Chaires, *Angew. Chem., Int. Ed.*, 2018, **57**, 7171–7175.
64 A. De Rache and J.-L. Mergny, *Biochimie*, 2015, **115**, 194–202.
65 P. Agrawal, C. Lin, R. I. Mathad, M. Carver and D. Yang, *J. Am. Chem. Soc.*, 2014, **136**, 1750–1753.
66 H. Li, in *G-Quadruplex Nucleic Acids. Methods in Molecular Biology*, ed. D. Yang and C. Lin, Humana, New York, NY, 2019, vol. 2035, pp. 105–116.
67 J. C. Martinez, J. Murciano-Calles, E. S. Cobos, M. Iglesias-Bexiga, I. Luque and J. Ruiz-Sanz, in *Applications of Calorimetry in a Wide Context – Differential Scanning Calorimetry, Isothermal Titration Calorimetry and Microcalorimetry*, ed. A. A. Elkordy, InTech, 2013, pp. 73–104.
68 D. Monchaud, C. Allain and M.-P. Teulade-Fichou, *Bioorg. Med. Chem. Lett.*, 2006, **16**, 4842–4845.
69 D. A. Megger, C. Fonseca Guerra, J. Hoffmann, B. Brutschy, F. M. Bickelhaupt and J. Müller, *Chem. – Eur. J.*, 2011, **17**, 6533–6544.
70 B. K. Teo, Y. H. Xu, B. Y. Zhong, Y. K. He, H. Y. Chen, W. Qian, Y. J. Deng and Y. H. Zou, *Inorg. Chem.*, 2001, **40**, 6794–6801.
71 S. Kroos and M. Hebenbrock, *Z. Kristallogr.*, 2024, **239**, 225–237.
72 J. E. M. Lewis, R. J. Bordoli, M. Denis, C. J. Fletcher, M. Galli, E. A. Neal, E. M. Rochette and S. M. Goldup, *Chem. Sci.*, 2016, **7**, 3154–3161.
73 F. Boisten, PhD thesis, Universität Münster, 2022.
74 C. Yu, K. H.-Y. Chan, K. M.-C. Wong and V. W.-W. Yam, *Chem. – Eur. J.*, 2008, **14**, 4577–4584.
75 R. B. Martin, *Science*, 1963, **139**, 1198–1203.
76 L. V. Le, T. J. Kim, Y. D. Kim and D. E. Aspnes, *Entropy*, 2022, **24**, 1238.
77 *APEX4 (Version 2021.10.0)*, Bruker AXS Inc., Madison, Wisconsin, USA, 2021.
78 (*a*) *SAINT (Version 8.40B, includes Xprep and SADABS)*, Bruker AXS Inc., Madison, Wisconsin, USA, 2001; (*b*) G. M. Sheldrick, *SADABS*, University of Göttingen, Germany, 1996.
79 G. M. Sheldrick, *Acta Crystallogr., Sect. A: Found. Adv.*, 2015, **71**, 3–8.
80 G. M. Sheldrick, *Acta Crystallogr., Sect. C: Struct. Chem.*, 2015, **71**, 3–8.
81 L. J. Farrugia, *J. Appl. Crystallogr.*, 2012, **45**, 849–854.
82 ORTEP-III – M. N. Burnett and C. K. Johnson, Oak Ridge Thermal Ellipsoid Plot Program for Crystal Structure Illustrations, Oak Ridge National Laboratory Report ORNL-6895, 1996.
83 M. J. Frisch, G. W. Trucks, H. B. Schlegel, G. E. Scuseria, M. A. Robb, J. R. Cheeseman, G. Scalmani, V. Barone, G. A. Petersson, H. Nakatsuji, X. Li, M. Caricato, A. V. Marenich, J. Bloino, B. G. Janesko, R. Gomperts, B. Mennucci, H. P. Hratchian, J. V. Ortiz, A. F. Izmaylov, J. L. Sonnenberg, D. Williams-Young, F. Ding, F. Lipparini, F. Egidi, J. Goings, B. Peng, A. Petrone, T. Henderson, D. Ranasinghe, V. G. Zakrzewski, J. Gao, N. Rega, G. Zheng, W. Liang, M. Hada, M. Ehara, K. Toyota, R. Fukuda, J. Hasegawa, M. Ishida, T. Nakajima, Y. Honda, O. Kitao, H. Nakai, T. Vreven, K. Throssell, J. J. A. Montgomery, J. E. Peralta, F. Ogliaro, M. J. Bearpark, J. J. Heyd, E. N. Brothers, K. N. Kudin, V. N. Staroverov, T. A. Keith,

R. Kobayashi, J. Normand, K. Raghavachari, A. P. Rendell, J. C. Burant, S. S. Iyengar, J. Tomasi, M. Cossi, J. M. Millam, M. Klene, C. Adamo, R. Cammi, J. W. Ochterski, R. L. Martin, K. Morokuma, O. Farkas, J. B. Foresman and D. J. Fox, *Gaussian 16, Revision C.01*, Gaussian, Inc., Wallingford, CT, 2016.

84 C. Adamo and V. Barone, *J. Chem. Phys.*, 1999, **110**, 6158–6170.

85 D. Andrae, U. Häußermann, M. Dolg, H. Stoll and H. Preuß, *Theor. Chim. Acta*, 1990, **77**, 123–141.

86 T. H. Dunning Jr. and P. J. Hay, in *Modern Theoretical Chemistry*, ed. H. F. Schaefer III, Plenum, New York, 1977, vol. 3, pp. 1–28.

87 J. Tomasi, B. Mennucci and R. Cammi, *Chem. Rev.*, 2005, **105**, 2999–3094.

88 S. Grimme, J. Antony, S. Ehrlich and H. Krieg, *J. Chem. Phys.*, 2010, **132**, 154104.

89 S. Grimme, S. Ehrlich and L. Goerigk, *J. Comput. Chem.*, 2011, **32**, 1456–1465.